Molecular Biology of the Cell
Vol. 11, 4033–4049, November 2000

Mutational Analysis Suggests That Activation of the Yeast Pheromone Response Mitogen-activated Protein Kinase Pathway Involves Conformational Changes in the Ste5 Scaffold Protein

Claudio Sette, Carla J. Inouye,* Shannon L. Stroschein,† Phillip J. Iaquinta, and Jeremy Thorner‡

Department of Molecular and Cell Biology, Division of Biochemistry and Molecular Biology, University of California, Berkeley, California 94720-3202

Submitted February 11, 2000; Revised August 25, 2000; Accepted September 7, 2000
Monitoring Editor: Tony Hunter

Ste5 is essential for pheromone response and binds components of a mitogen-activated protein kinase (MAPK) cascade: Ste11 (MEKK), Ste7 (MEK), and Fus3 (MAPK). Pheromone stimulation releases G$\beta\gamma$ (Ste4-Ste18), which recruits Ste5 and Ste20 (p21-activated kinase) to the plasma membrane, activating the MAPK cascade. A RING-H2 domain in Ste5 (residues 177–229) negatively regulates Ste5 function and mediates its interaction with G$\beta\gamma$. Ste5(C177A C180A), carrying a mutated RING-H2 domain, cannot complement a *ste5*Δ mutation, yet supports mating even in *ste4*Δ *ste5*Δ cells when artificially dimerized by fusion to glutathione *S*-transferase (GST). In contrast, wild-type Ste5 fused to GST permits mating of *ste5*Δ cells, but does not allow mating of *ste4*Δ *ste5*Δ cells. This differential behavior provided the basis of a genetic selection for *STE5* gain-of-function mutations. *MAT*a *ste4*Δ *ste5*Δ cells expressing Ste5-GST were mutagenized chemically and plasmids conferring the capacity to mate were selected. Three independent single-substitution mutations were isolated. These constitutive *STE5* alleles induce cell cycle arrest, transcriptional activation, and morphological changes normally triggered by pheromone, even when G$\beta\gamma$ is absent. The first, Ste5(C226Y), alters the seventh conserved position in the RING-H2 motif, confirming that perturbation of this domain constitutively activates Ste5 function. The second, Ste5(P44L), lies upstream of a basic segment, whereas the third, Ste5(S770K), is situated within an acidic segment in a region that contacts Ste7. None of the mutations increased the affinity of Ste5 for Ste11, Ste7, or Fus3. However, the positions of these novel-activating mutations suggested that, in normal Ste5, the N terminus may interact with the C terminus. Indeed, in vitro, GST-Ste5(1-518) was able to associate specifically with radiolabeled Ste5(520-917). Furthermore, both the P44L and S770K mutations enhanced binding of full-length Ste5 to GST-Ste5(1-518), whereas they did not affect Ste5 dimerization. Thus, binding of G$\beta\gamma$ to the RING-H2 domain may induce a conformational change that promotes association of the N- and C-terminal ends of Ste5, stimulating activation of the MAPK cascade by optimizing orientation of the bound kinases and/or by increasing their accessibility to Ste20-dependent phosphorylation (or both). In accord with this model, the novel Ste5 mutants copurified with Ste7 and Fus3 in their activated state and their activation required Ste20.

INTRODUCTION

The pheromone response pathway of the yeast *Saccharomyces cerevisiae* has provided a system for elucidating mechanisms that convert an extracellular signal into both a morphological response and a change in the pattern of gene expression (reviewed in Bardwell *et al.*, 1994; Leberer *et al.*, 1997a). Mating of haploid cells (*MAT***a** and *MAT*α) requires the action of peptide pheromones: *MAT***a** cells secrete **a**-factor, and *MAT*α cells secrete α-factor. The cell surface receptors for these peptides (Ste2 in *MAT***a** cells binds α-factor, and Ste3 in *MAT*α cells binds **a**-factor) are members of the superfamily of seven-transmembrane-segment receptors and are coupled to a heterotrimeric G protein. Pheromone

Present addresses: *c/o Tjian Laboratory, Howard Hughes Medical Institute, Department of Molecular and Cell Biology, Koshland Hall, University of California, Berkeley, California 94720-3204; †c/o Luo Laboratory, Life Sciences Division, Lawrence Berkeley National Laboratory, Donner Laboratory, Berkeley, California 94720-3206.
‡ Corresponding author. E-mail address: jeremy@socrates.berkeley.edu.

binding to its cognate receptor triggers dissociation of the associated Gα subunit (Gpa1) from the Gβγ complex (Ste4-Ste18). Released Gβγ complexes initiate activation of a signal transduction pathway that involves, among other components, an evolutionarily conserved module consisting of three tiers of protein kinases: a MEKK (Ste11), a MEK (Ste7), and two mitogen-activated protein kinases (MAPKs) (Fus3 and Kss1) (reviewed in Gustin *et al.*, 1998; Posas *et al.*, 1998). Activation of this cascade leads to MAPK-dependent phosphorylation of substrates required for pheromone response, including Ste12, a transcription factor required for induction of pheromone-responsive genes (Song *et al.*, 1991; Elion *et al.*, 1993; Hung *et al.*, 1997); Dig1 and Dig2, negative regulators of Ste12 (Cook *et al.*, 1996; Tedford *et al.*, 1997); and, Far1 (Peter *et al.*, 1993), a protein involved in both inhibition of the G1-cyclin-bound forms of the cyclin-dependent kinase Cdc28 (Tyers and Futcher, 1993; Peter and Herskowitz, 1994), and in morphological changes that polarize the actin cytoskeleton toward the side of the cell facing the highest pheromone concentration (Valtz *et al.*, 1995; Butty *et al.*, 1998). As a result, cells arrest in the G_1 phase of the cell cycle, form a protrusion ("shmoo tip") toward its mating partner, and express the proper subset of gene products required for efficient conjugation (Erdman *et al.*, 1998; Madhani *et al.*, 1999; Roberts *et al.*, 2000).

Although release of Gβγ is sufficient to activate the pathway, it is not completely understood how this event is linked to activation of the MAPK cascade. Two additional proteins are required for pheromone response. One is Ste20 (Leberer *et al.*, 1992; Ramer and Davis, 1993), a protein kinase homologous to the p21-activated kinases (PAKs) (Manser and Lim, 1999). The other is Ste5, a protein thought to dictate the specificity and efficiency of signaling by serving as a scaffold that physically associates with Ste11, Ste7, and the MAPKs (Choi *et al.*, 1994; Marcus *et al.*, 1994; Printen and Sprague, 1994), thereby also insulating from inappropriate activation certain of the components, such as Ste11 and Ste7, that are shared by other signaling pathways (Yashar *et al.*, 1995; Posas and Saito, 1997). A mechanism that links free Gβγ directly to activation of the MAPK cascade is suggested by recent findings that the released Gβγ complex can interact with both Ste5 (Whiteway *et al.*, 1995; Inouye *et al.*, 1997b; Pryciak and Huntress, 1998) and Ste20 (Leeuw *et al.*, 1998). The surfaces on Gβ that mediate these two interactions are different, but juxtaposed (Leeuw *et al.*, 1998; Dowell *et al.*, 1999). Because the Gβγ complex released from pheromone receptors remains anchored to the plasma membrane via both prenylation and palmitoylation of the C terminus of Gγ (Hirschman and Jenness, 1999; Manahan *et al.*, 2000), Gβγ association with both Ste5 and Ste20 recruits these proteins to the plasma membrane (Pryciak and Huntress, 1998; Mahanty *et al.*, 1999; Dhillon *et al.*, 2000) where their proximity facilitates functional interaction and leads to activation of the MAPK cascade tethered to Ste5. This model is supported by the fact that mutations in either Ste5 (Inouye *et al.*, 1997b; Feng *et al.*, 1998) or Ste20 (Leeuw *et al.*, 1998) that alter only their ability to bind to Ste4 (Gβ) cause sterility in vivo.

Although it has been reported that Ste20-mediated phosphorylation of Ste11 (MEKK) does not enhance the in vitro catalytic activity of Ste11 (Wu *et al.*, 1995) and that Ste11 (as a glutathione *S*-transferase [GST] fusion) displays the same level of activity (with Ste7 as substrate) when isolated from either naive or pheromone-treated cells (Neiman and Herskowitz, 1994), it now seems clear that phosphorylation of specific residues in the N terminus of Ste11 by Ste20 is required for activation of the MAPK cascade (Drogen *et al.*, 2000). However, there is evidence that Ste5 also plays an active role in MAPK activation and does not merely serve as a passive scaffold. We identified a point mutation in Ste5 that could stimulate signaling, even in the absence of receptor activation (Hasson *et al.*, 1994). This mutation, Ste5(T52M), lies near the N terminus just upstream of a stretch of basic residues in a region not known to associate with any interacting protein (Elion, 1995; Inouye *et al.*, 1997a) (Figure 1A). Another mutant, Ste5(C177A C180A), in which two consensus Zn^{2+}-binding residues in the RING-H2 domain of Ste5 have been eliminated, is unable to interact with Ste4 and is unable to support mating of *ste5*Δ cells; however, if artificially dimerized via fusion to GST (Maru *et al.*, 1996), the Ste5(C177A C180A)-GST chimera is not only functional but also overcomes the need for Gβγ because it can support mating even in *ste4*Δ *ste5*Δ cells (Inouye *et al.*, 1997b). This constitutive activation of the pheromone response pathway suggests that, normally, free Gβγ released from pheromone-occupied receptors associates with Ste5 and causes some conformational change that facilitates activation of the MAPK cascade. Both biochemical (Yablonski *et al.*, 1996; Feng *et al.*, 1998) and genetic (Inouye *et al.*, 1997a,b) methods indicate that Ste5 exists as an oligomer. Deletion analysis located regions important for this Ste5-Ste5 self-association to two segments: residues 138–239 (which overlap with the RING-H2 domain) and/or 335–586 (Yablonski *et al.*, 1996). Although multimerization of Ste5 may be necessary for signaling, it is not sufficient because, unlike Ste5(C117A C180A)-GST, wild-type Ste5-GST does not complement *ste4*Δ *ste5*Δ cells (Inouye *et al.*, 1997b). Thus, alteration of the RING-H2 (either by mutation or via interaction with Gβγ) must alleviate some negative constraint in Ste5 that promotes signaling via a mechanism different from (or in addition to) oligomerization.

To gain more insight into the role that Ste5 plays in activation of the MAPK cascade, we sought to identify additional gain-of-function alleles in Ste5. In this study, we used a new positive selection to obtain novel constitutively active derivatives of Ste5. We selected for mutations that, like alteration of the RING-H2 motif, permit Ste5-GST to function in the absence of Gβγ. Here we present a detailed phenotypic and biochemical characterization of these novel alleles. The nature of these mutations confirmed, first, that the RING-H2 domain in Ste5 exerts some negative constraint on the overall structure of Ste5 that, when alleviated, permits signal propagation. Second, the positions of these mutations suggested that the N terminus and the C terminus of Ste5 can associate, and we present direct physical evidence for this interaction.

MATERIALS AND METHODS

Strains and Growth Conditions

Strains used in this study are listed in Table 1. Strain BYB88 (*ste4*Δ *ste5*Δ) has been described previously (Inouye *et al.*, 1997b). To generate strain YCS1 (*ste4*Δ *ste5*Δ *ste20*Δ), one-step gene transplacement (Rothstein, 1983) was accomplished by DNA-mediated transformation of strain BYB88 with a *ste20*Δ::LEU2 cassette that is de-

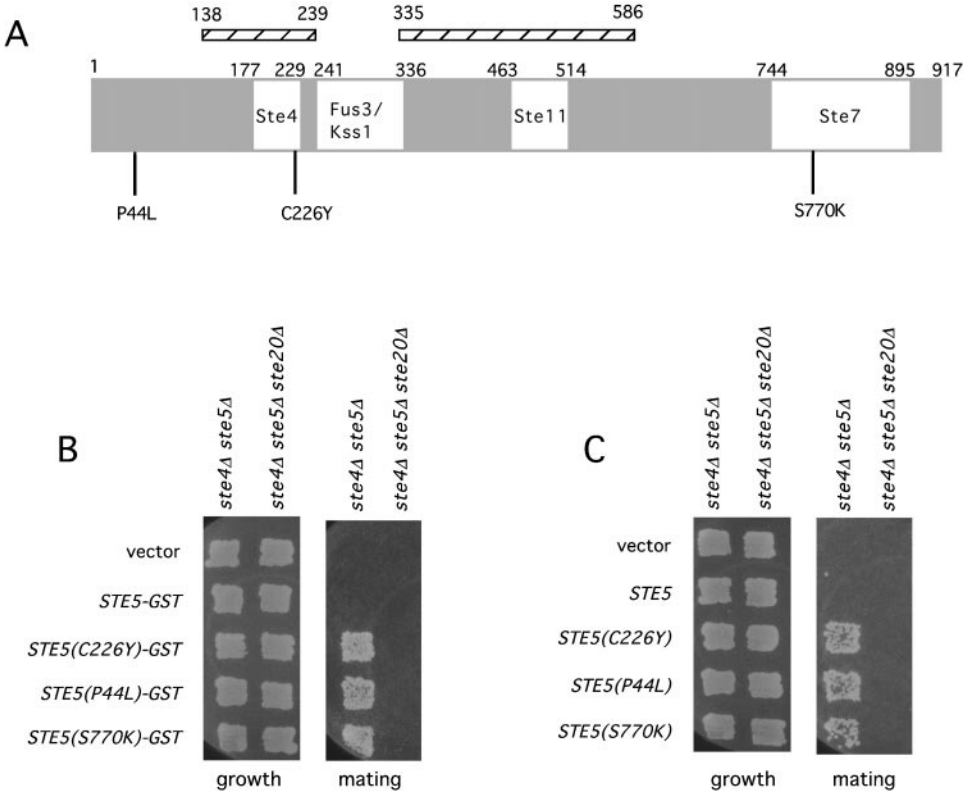

Figure 1. Positions of mutations that constitutively activate *STE5*. (A) Schematic representation of the primary structure of the 917-residue Ste5 polypeptide (gray box). Regions of Ste5 implicated in the binding of the indicated proteins (white boxes) and segments of Ste5 implicated in Ste5 oligomerization (hatched lines) are shown. Positions of the single-substitution mutations isolated by chemical mutagenesis of Ste5-GST are indicated below the gray box: P44L, C226Y, and, S770K. (B) G$\beta\gamma$-independent mating phenotype of the activated *STE5* alleles. (C) Requirement for Ste20 function. Otherwise isogenic *MAT***a** strains of the indicated genotype (either *ste4*Δ *ste5*Δ or *ste4*Δ *ste5*Δ *ste20*Δ) were transformed with either empty vector or the same vector expressing either wild-type Ste5-GST or wild-type Ste5, Ste5(C226Y)-GST or Ste5(C226Y), Ste5(P44L)-GST or Ste5(P44L), or Ste5(S770K)-GST or Ste5(S770K), as indicated, and patch mating assays were carried out as described in MATERIALS AND METHODS. Cells were pregrown on SCRaf plates ("growth"), replica-plated onto YPGal plates spread with the *MAT*α tester and incubated for 6 h, and then replica-plated onto minimal medium selective for diploids ("mating").

scribed in detail elsewhere (Ramer and Davis, 1993). To generate strain YCS3 (*ste4*Δ *ste5*Δ *ste12*Δ), plasmid pLB1367 (gift from Dr. Gustav Ammerer, University of Vienna, Austria), containing a 1133-bp internal deletion of *STE12* replaced by the *LEU2* gene, was digested with *Bam*HI, and the resulting gel-purified DNA fragment was used for transformation of strain BYB88. Disruption of chromosomal loci was confirmed by polymerase chain reaction (PCR) amplification of DNA isolated from transformants and parental cells by using appropriate primers.

Isolation of STE5 Gain-of-Function Alleles by Chemical Mutagenesis

Yeast strain BYB91 (*MAT***a** *ste4*Δ *ste5*Δ) (Table 1) was transformed with pCJ148, a *URA3*-marked *CEN* plasmid expressing a $(His)_6$- and c-Myc epitope-tagged derivative of *STE5-GST* under control of the *GAL1* promoter. A culture (10 ml) of this transformant was grown in a synthetic complement medium containing 2% glucose and supplemented with all of the amino acids, but lacking uracil (SCGlc-Ura) (Sherman *et al.*, 1986) to an $A_{600\ nm} = 0.5$ ($\sim 5 \times 10^6$ cells/ml), washed twice with 50 mM K-PO_4 (pH 7.4), and resuspended in 30 ml of the same buffer. Samples (7.5 ml) of the suspension were distributed to four tubes, two of which received 150 μl of ethylmethane sulfonate (EMS), whereas the other two served as controls. After incubation for 1 h at 30°C with gentle vortex mixing every 10 min, 7.5 ml of 10% Na-thiosulfate was added to each tube to quench the mutagen and cells were collected by centrifugation at 1000 $\times$ *g* for 5 min. The resulting pellets were washed twice with 50 mM K-PO_4 (pH 7.4), and resuspended in 1 ml of the same buffer. Samples (100–150 μl) of appropriate dilutions (10^{-4} for EMS-treated cells and 10^{-6} for the untreated controls) of the final cell suspensions were each plated on fifteen 150-mm-diameter agar plates containing SCGlc-Ura medium and incubated at 30°C for 3 d. As determined by comparing the number of viable colonies yielded by

Table 1. *Saccharomyces cerevisiae* strains used

Strain	Genotype	Source
BYB84	*MAT***a** *gal2 leu2 prb1-1122 pep4-3 prc1-407 trp1 ura3-52 ste5*Δ	Inouye *et al.* (1997b)
BYB88	*MAT***a** *ade2-101^{oc} his3-*Δ*200 leu2*Δ*-1 lys2-801^{am} trp1-*Δ*63 ura3-52 ste4*Δ*::TRP1 ste5*Δ*::LYS2*	Inouye *et al.* (1997b)
BYB91	*MAT***a** *ade2-1 can1-100 his3-11,15 leu2-3,112 lys2::hisG trp1-1 ura3-1 ste4*Δ*::TRP1 ste5*Δ*::LYS*	This work
YCS1	*MAT***a** *ade2-101^{oc} his3-*Δ*200 leu2*Δ*-1 lys2-801^{am}trp1-*Δ*63 ura3-52 ste4*Δ*::TRP1 ste5*Δ*::LYS2 ste20*Δ*::LEU2*	This work
YCS3	*MAT***a** *ade2-101^{oc} his3-*Δ*200 leu2*Δ*-1 lys2-801^{am}trp1-*Δ*63 ura3-52 ste4*Δ*::TRP1 ste5*Δ*::LYS2 ste12*Δ*::LEU2*	This work
DC17	*MAT*α *his1*	J.B. Hicks

the EMS-treated samples to those on the control plates, the mutagenesis resulting in 70–75% killing. Each of the 30 plates resulting from the EMS treatment was replica-plated on a rich medium containing 2% galactose (YPGal) (Sherman *et al.*, 1986), which had been seeded previously with a suspension of a tester strain of opposite mating type (DC17), and incubated overnight at 30°C. The mating plates were then replica-plated to an appropriate minimal medium (SGlc) to select the resulting diploids. Plasmid DNA was rescued from the 44 initial candidates obtained and retested for galactose-dependent induction of mating competence by the same procedure in a different *ste4*Δ *ste5*Δ strain (BYB88). Three plasmids (pSL1, pSL2, and pSL3) reproducibly conferred mating ability in both BYB91 and BYB88 in a plasmid- and galactose-dependent manner and were chosen for further study.

Mating Assay

Mating proficiency was assessed by replica-plating patches of the *MAT***a** cells to be tested onto a lawn of the *MAT*α tester strain (DC17) on YPGal plates (Sprague, 1991). After incubation overnight at 30°C, the mating plates were replica-plated onto plates containing synthetic minimal medium selective for diploids and incubated at 30°C for 2 to 3 d.

Measurement of Growth Rate and Examination of Morphology

Strains harboring plasmids expressing wild-type or mutant Ste5 (or the corresponding Ste5-GST and/or Ste5-GFP derivatives) from the *GAL1* promoter were grown at 30°C in SC medium containing 2% raffinose (SCRaf) to an $A_{600\ nm} = 0.2$. Expression was induced by addition of galactose to the medium to a final concentration of 2%, and the cultures were incubated at the same temperature for additional 8 h. At 2-h intervals, samples were withdrawn and cell number was counted in a hemocytometer chamber under the phase-contrast microscope. Likewise, samples under coverslips on standard microscope slides were also examined under the phase-contrast microscope or the fluorescence microscope (see below) to monitor the morphology of the cells. To examine the pattern of chitin deposition, cells were washed once in phosphate-buffered saline (PBS), fixed in 5% formaldehyde for 30 min at room temperature, and stained with 0.1 mg/ml Calcofluor White (Sigma, St. Louis, MO) for 30 min at room temperature (Pringle *et al.*, 1991). Cells were examined under a Zeiss epifluorescence microscope by using the 100× objective. Images were collected by using a Sony charged-coupled device camera and digitally recorded using imaging software (Phase3; Northern Exposure, Inc., Milford, MA) and Photoshop (Adobe Systems, Inc., Mountain View, CA).

Plasmid Constructions and Recombinant DNA Methods

Escherichia coli strain DH5α (Hanahan, 1983) was used for routine manipulation and propagation of plasmids. Standard molecular biology techniques were used for plasmid construction (Sambrook *et al.*, 1989). Unless otherwise indicated, all PCR reactions used native *Pfu* DNA polymerase (Stratagene, La Jolla, CA). Plasmid pCJ174 was constructed by inserting the *ste5(C177A C180A)* allele (Inouye *et al.*, 1997b) into the *Bam*HI site in a derivative of the *CEN*-based, *LEU2*-marked, *GAL1*-promoter containing vector YCpLG, which has been described previously (Bardwell *et al.*, 1998), in which the *Eco*RI site in the polylinker was removed by digestion with *Eco*RI, filling in with Klenow fragment of *E. coli* DNA polymerase I, and religation. The fragment inserted contained a *Bam*HI site just upstream of the *STE5* ATG initiator codon, introduced by PCR as described in detail elsewhere (Inouye *et al.*, 1997a), and a native *Bam*HI site that lies 265 bp downstream of the TAG stop codon of the *STE5* open reading frame. Plasmids pCJ6 and pCJ148 have been described previously (Inouye *et al.*, 1997a,b). Plasmids pSL1, pSL2, and pSL3 are all derived from pCJ148 by EMS treatment as described above and the *STE5* coding sequence in each of them was determined by standard dideoxynucleotide chain-termination methods (Biggin *et al.*, 1983). Plasmids pCS22, pCS7, and pCS8, carrying *STE5(C226Y)*, *STE5(P44L)*, and *STE5(S770K)*, respectively, under control of the *GAL1* promoter on a 2-μm DNA plasmid, were constructed by replacing the *Kpn*I-*Xho*I fragment containing the *STE5* coding region in pCJ6 with the corresponding fragments from pSL1, pSL2, and pSL3, respectively. YEpL-FUS1Z (gift from J. Shimoni, this laboratory) is a *LEU2*-marked, 2-μm DNA-containing plasmid carrying a fusion of the *FUS1* promoter to the *E. coli lacZ* gene, and was constructed by excising the *URA3* gene from plasmid, YEpU-Fus1Z (Bardwell *et al.*, 1998), by digestion with *Sse*8387I and *Sma*I and substituting the *LEU2* gene, which was obtained by cleavage of plasmid pJJ282 (Jones and Prakash, 1990) with *Pst*I and *Sma*I. Plasmid pCJ80, which expresses from the *GAL1* promoter an in-frame fusion of a brightness-enhancing variant of green fluorescent protein (GFP) to the C terminus of Ste5, is described in detail elsewhere (Dhillon *et al.*, 2000). Plasmids pCS49, pCS18, and pCS50 encoding Ste5(C226Y)-GFP, Ste5(P44L)-GFP, and Ste5(S770K)-GFP, respectively, were obtained by replacing the *Kpn*I-*Xho*I fragment of the *STE5* sequence in pCJ80 with the corresponding fragments from plasmids pSL1, pSL2, and pSL3. Overexpression of *STE7* from plasmid YCpLG-STE7 under control of the *GAL1* promoter has been described before (Inouye *et al.*, 1997a). To prepare pCS11 and pCS26, the region of *STE5* corresponding to codons 1–518 was amplified by using *Pfu* DNA polymerase, a 5′-primer containing a *Bam*HI site, a 3′-primer containing a *Xho*I site, and pCJ148 DNA as template for wild-type *STE5* or pSL2 DNA as template for the *STE5(P44L)* mutant. The resulting PCR products were cloned into pGEX5X-2 (Pharmacia, Piscataway, NJ) generating in-frame fusions to GST. To prepare pCS19 and pCS27, the region of *STE5* corresponding to codons 520–917 was amplified in the same manner by using a 5′ primer containing an *Eco*RI site, a 3′ primer containing a *Sac*I site, and pCJ148 DNA as template for wild-type *STE5* or pSL3 DNA as template for the *STE5(S770K)* mutant. The resulting fragments were cloned into the vector GEM4Z (Promega, Madison, WI) for in vitro transcription-translation, as described below.

Subcellular Localization of Wild-type and Mutant Ste5 Proteins by Using GFP

Strains BYB84 (*ste5*Δ) or BYB88 (*ste4*Δ *ste5*Δ) were transformed with plasmids encoding fusions of GFP to the C terminus of either wild-type Ste5 (pCJ80), Ste5(C226Y) (pCS49), Ste5(P44L) (pCS18), or Ste5(S770K) (pCS50), in the presence or absence of a second plasmid expressing the same wild-type or mutant derivative of Ste5-GST (pCJ148, pSL1, pSL2, and pSL3, respectively). The transformants were grown in SCRaf medium to an $A_{600\ nm} = 0.6$, and then expression of the GFP fusions (and GST fusions) was induced by addition of galactose (2% final concentration) to the cultures. After 2 h, *ste5*Δ cells were washed in SCGlc to repress further expression of the chimeras. Cultures of the *ste4*Δ *ste5*Δ cells were induced for 4–6 h with galactose to induce morphological changes, and examined thereafter under a fluorescence microscope equipped with an appropriate cut-off filter. Cultures of the *ste5*Δ cells were divided into two equal portions, one of which was treated for 30–60 min with 12 μM α-factor, as previously described (Dhillon *et al.*, 2000), and the other was left untreated, as a control. Immediately thereafter, the cells were examined under the fluorescence microscope. Images were collected as described above.

Immunoprecipitation and Immunoblotting

Strain expressing from plasmids either wild-type or mutant *STE5* (or *STE5-GST*) under control of the *GAL1* promoter were pregrown at 30°C in SCRaf to an $A_{600\ nm} = 0.6$ under conditions selective for maintenance of the plasmids. Expression was induced by addition of galactose (2% final concentration) and incubation for 3 h. Cells

were harvested, washed once with PBS, and lysed by vigorous vortex mixing with chilled glass beads in ice-cold lysis buffer (20 mM Tris-HCl, pH 7.2, 12.5 mM K-acetate, 4 mM $MgCl_2$, 0.5 mM EDTA, 5 mM sodium bisulphite, 0.1% Tween 20, 12.5% glycerol) containing 1 mM dithiothreitol, 10 mM Na-β-glycerophosphate, 0.5 mM $NaVO_4$, 2 μg/ml leupeptin, 2 μg/ml pepstatin A, 1 mM benzamidine, 2 μg/ml aprotinin, and 1 mM freshly prepared phenylmethylsulfonyl fluoride. The resulting crude extracts were clarified by centrifugation at 30,000 $\times$ *g* in a microcentrifuge for 10 min at 4°C. Based on determination of the protein concentration in these supernatant fractions by using a commercial kit (Bio-Rad, Hercules, CA), a volume of each soluble fraction containing 1 mg of protein total was preadsorbed for 30–60 min with 40 μl of a 50:50 slurry of Protein A/G-agarose beads (Calbiochem, La Jolla, CA) and then the beads were removed by brief centrifugation in a microfuge. To the resulting supernatant fraction was added 1 μl of mouse ascites fluid containing an anti-c-Myc monoclonal antibody, 9E10 (Evan *et al.*, 1985), and another aliquot of Protein A/G-agarose beads. For the experiments in which Ste5 multimerization was assessed, a sample (1 μg) of a commercial polyclonal anti-GST antibody (Santa Cruz Biotechnology, Santa Cruz, CA) was used to capture Ste5-GST chimeras. The resulting mixtures were incubated with rotatory agitation for 2 h at 4°C, and then the bead-bound immune complexes were collected by brief centrifugation, washed three times (500 μl each) with ice-cold lysis buffer containing 0.1 mg/ml bovine serum albumin, and then twice with ice-cold 50 mM Tris-HCl, pH 7.4, containing the same protease and phosphatase inhibitors indicated above. The immune complexes were solubilized by resuspending the beads in SDS-PAGE sample buffer and boiling for 5 min. Eluted proteins were resolved by SDS-PAGE, transferred electrophoretically to an Immobilon-P membrane filter (Millipore, Bedford, MA) by using a semidry transfer cell (Bio-Rad), and analyzed by immunoblotting. Filters were incubated with the appropriate primary antibodies for 90 min at room temperature, followed by incubation with the appropriate horseradish peroxidase-conjugated secondary antibodies for 60 min at room temperature, and then visualized by using a commercial chemiluminescence detection system (Santa Cruz Biotechnology). The anti-Ste7 and anti-Ste11 antibodies (Cairns *et al.*, 1992), and the anti-Fus3 antibodies (Brill *et al.*, 1994), are described in the references cited. Polyclonal anti-GFP antibodies were obtained from Boehringer-Mannheim (Indianapolis, IN).

Immune-Complex Kinase Assay of Fus3 Activity

Myc-tagged wild-type or mutant Ste5 constructs were immunoprecipitated as described immediately above. The bead-bound Ste5 and associated proteins were washed three times (500 μl each) with ice-cold lysis buffer containing 0.1 mg/ml bovine serum albumin and then twice (500 μl each) in kinase buffer (50 mM Tris-HCl, pH 7.4, 20 mM $MgCl_2$, 5 mM EGTA, 1 mM dithiothreitol, 10 mM Na-β-glycerophosphate, 0.5 mM $NaVO_4$). The suspension of beads was split into two equal portions, and one was used for immunoblot blot analysis, as described above, and the other was used for enzyme assay, as follows. Fus3 activity was measured as the amount of radioactivity incorporated into a specific substrate, GST-Ste7(1-172) (Bardwell *et al.*, 1996). Kinase reactions were initiated by resuspending the bead-bound immune complex in 30 μl of kinase buffer containing 100 μM [γ-^{32}P]ATP (3.3 mCi/μmol) and 1 mg of purified GST-Ste7(1-172) and incubated at 30°C for 20 min with occasional shaking of the tubes to disperse the beads. To terminate the reaction, beads were removed by centrifugation and the supernatant fraction was decanted into a fresh tube containing SDS-PAGE sample buffer and boiled for 5 min. Proteins were resolved by SDS-PAGE on a 10% slab gel, which was dried and analyzed by autoradiography using X-ray film. Densitometric analysis of bands in autoradiograms and fluorograms was performed by using public-domain imaging software available from the National Institutes of Health.

In Vitro Transcription-Translation and Analysis of Protein–Protein Interaction

Fus3 and Ste5(520-917) were produced by using a commercial SP6 RNA polymerase-dependent coupled transcription-translation kit (TNT; Promega), according to the manufacturer's instructions. The resulting ^{35}S-labeled proteins were incubated with rotatory agitation for 1 h at 4°C with excess glutathione-agarose beads that had been preadsorbed with either GST or GST-Ste5(1-518). The beads were washed three times with PBS, and then eluted with 5 mM freshly prepared reduced glutathione in 50 mM Tris-HCl (pH 8.0). The resulting eluates were diluted into SDS sample buffer, boiled for 5 min, and resolved by SDS-PAGE on a 12% slab gel, which was dried and analyzed by autoradiography using X-ray film. For the kind of experiment shown in Figure 9A, bacterially-expressed GST, GST-Ste5(1-518), or GST-Ste5^{P44L}(1-518) fusion proteins were adsorbed to agarose-beads as above. Beads were then incubated with extracts of strain BYB88 (*MAT***a** *ste4*Δ *ste5*Δ) expressing c-Myc-epitope-tagged versions of either full-length wild-type Ste5, Ste5(P44L), or Ste5(S770K) for 90 min at 4°C under constant agitation. Beads were washed and bead-bound proteins were eluted as described above. Eluted proteins were resolved by SDS-PAGE and analyzed by staining with Coomassie blue (to examine the loading of GST or GST fusion proteins) or by immunoblotting with appropriate antisera.

RESULTS

Isolation of Constitutively Active G$\beta\gamma$-independent Alleles of STE5 *by Random Chemical Mutagenesis*

We have shown previously that expression of a Ste5(C177A C180A)-GST chimera in *ste4*Δ *ste5*Δ cells rescues mating ability, whereas a wild-type Ste5-GST chimera does not (Inouye *et al.*, 1997b). We realized that this difference could be exploited as the basis for an unbiased and more general selection for additional gain-of-function alleles of *STE5*. We searched after random mutagenesis of Ste5-GST with EMS for mutations that, like alteration of the RING-H2 motif, permitted Ste5-GST to function in the absence of G$\beta\gamma$. Three independently isolated *STE5* alleles were recovered (Figure 1A) that reproducibly conferred proficient mating in the absence of G$\beta\gamma$ (Figure 1B). Nucleotide sequence analysis revealed that each allele contained a different single-residue substitution.

The mutation (C226Y) in the first allele changes the seventh conserved Zn^{2+}-binding residue of the RING-H2 motif. Because the RING-H2 domain mutations we studied previously were generated by site-directed mutagenesis of the first and/or second Zn^{2+}-binding residue (Inouye *et al.*, 1997b), isolation of C226Y provided independent confirmation that perturbation of the RING-H2 domain activates Ste5 function (at least in the context of its fusion to GST). The mutation (P44L) in the second allele was also particularly interesting because it is situated just proximal to a strikingly basic segment ($P^{44}x_2RxKKx_3Kx_2Rx_2Rx_3KKKR^{67}$) near the N terminus of Ste5. Moreover, the P44L substitution lies just upstream of the position of the point mutation (T52 M) that we isolated previously by hydroxylamine mutagenesis, which partially activated Ste5 function (and did not require the context of a GST fusion) (Hasson *et al.*, 1994). The mutation (S770K) in the third allele was also striking because it lies just proximal to a very acidic segment ($S^{770}x_5DExDDDDEEDxDDx_2DxExD^{785}$) near the C terminus of Ste5. Moreover, S770K was identical to one of the alter-

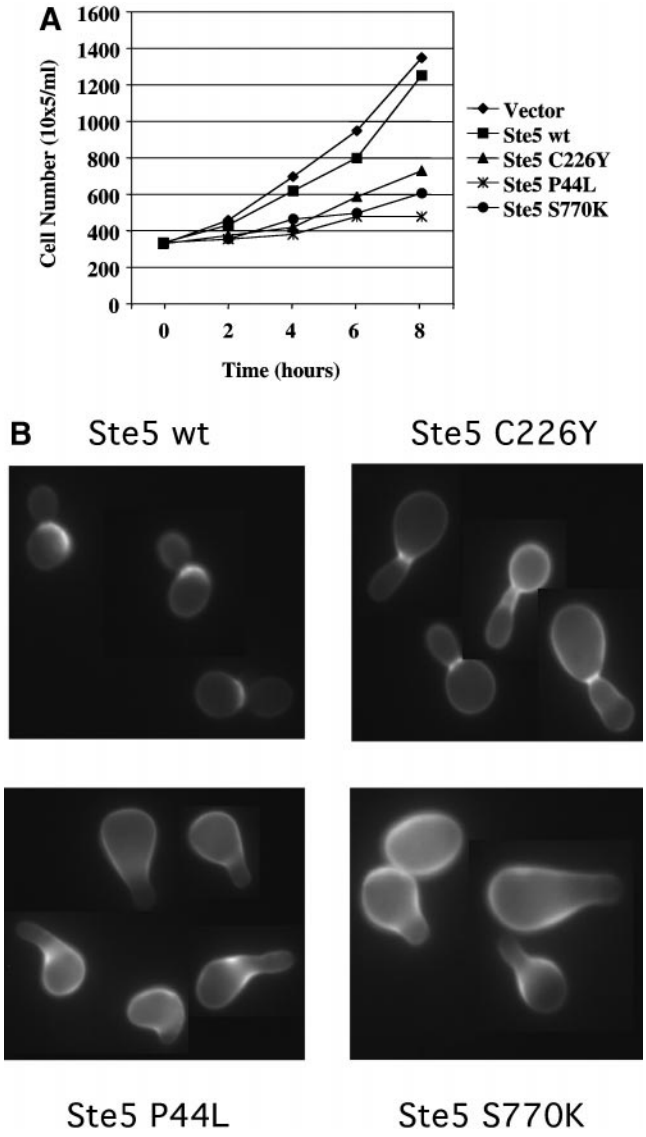

Figure 2. Activated *STE5* alleles cause G_1 arrest and induce morphological changes. (A) A *ste4*Δ *ste5*Δ strain carrying an empty vector or the same vector expressing either wild-type Ste5-GST or the indicated activated mutant derivatives (as GST fusions), under the control of the *GAL1* promoter were pregrown in SCRaf to an $A_{600\ nm} = 0.2$, and then galactose (2% final concentration) was added to induce expression of the proteins. At the indicated times, triplicate samples of the cultures were removed and cell number was determined as described in MATERIALS AND METHODS; values plotted represent the average (SD was <10%). (B) Samples of the cultures shown in A were removed 6 h after addition of galactose, fixed for 30 min in 5% formaldehyde at room temperature, washed in PBS, stained for 30 min at room temperature with Calcofluor, spotted on glass slides, mounted with a coverslip, and examined under the fluorescence microscope, as described in MATERIALS AND METHODS.

ations (I568T S770K) in an allele that activated Ste5 function in the absence of its fusion to GST, which was isolated in an independent PCR-based mutagenesis and screen (our unpublished results).

To determine whether the constitutive phenotype conferred by these three substitution mutations required their fusion to GST, each of these alleles was transferred into a 2-μm DNA plasmid expressing otherwise native *STE5* from the *GAL1* promoter and tested for its ability to confer G$\beta\gamma$-independent mating (Figure 1C). Unlike wild-type *STE5* expressed from the same vector, all three mutants were able to rescue the mating ability of *ste4*Δ *ste5*Δ cells (Figure 1C), although somewhat less efficiently than the corresponding GST fusions, which were expressed from the *GAL1* promoter on a *CEN* plasmid (Figure 1B). Thus, each mutation clearly contributes to the constitutively active phenotype, even in the absence of fusion to GST. In such qualitative patch mating assays, Ste5(C226Y) mated at a frequency that was reproducibly higher than that displayed by Ste5(C177A C180A) (our unpublished results). We have previously determined, by using quantitative mating assays, that, under the same conditions (expression from the *GAL1* promoter on a 2-μm DNA vector), Ste5(C177A C180A) mates with an efficiency of $\sim 2 \times 10^{-4}$ compared with $<10^{-6}$ for *ste5*Δ cells (Inouye *et al.*, 1997b). On this basis, we estimate that cells expressing Ste5(C226Y) mate at a frequency that may approach 1% of the efficiency of wild-type cells.

Phenotypic Characterization of the Activated STE5 Alleles

Stimulation of the pheromone-signaling pathway elicits a variety of cellular responses. To assess the relative strength of the three single-substitution alleles and to determine whether they displayed any differential effects, various aspects of cellular response were assayed. First, the ability of the three mutants to impose G1-specific cell cycle arrest was examined by inducing expression of the mutants (as GST fusions from a *CEN* vector under control of the *GAL1* promoter) in *MAT***a** *ste4*Δ *ste5*Δ cells pregrown on raffinose (or, in some experiments, on glucose) by addition of galactose and following both growth rate (Figure 2A) and cell morphology (Figure 2B). When grown on glucose or raffinose, all transformants (vector alone, Ste5-GST, and each of the three mutants) grew at the same rate (our unpublished results). After addition of galactose, cells carrying the vector alone or expressing wild-type Ste5-GST continued to grow at a nearly identical rate and went through two doublings in the 8-h time period. Likewise, the same cells overexpressing native Ste5 (not as a GST fusion) continued to grow normally, due to the absence of G$\beta\gamma$ (our unpublished results). In contrast, expression of Ste5(P44L)-GST and also Ste5(S770K)-GST caused the *ste4*Δ *ste5*Δ cells to cease growth for nearly the entire 8-h period. Expression of the Ste5(C266Y)-GST allele caused a significant lag (4–5 h) before the cells were able to resume growth, but was reproducibly less potent than Ste5(P44L)-GST or Ste5(S770K)-GST in retarding cell cycle progression. This cell cycle arrest was due to activation of the pheromone response pathway, and not the result of overexpression of "toxic" proteins because none of the three mutant Ste5-GST proteins had any detectable affect on the rate of growth of *ste12*Δ cells or *fus3*Δ *kss1*Δ cells after shift to galactose medium, even though all three proteins were produced at levels indistinguishable from those generated in *ste4*Δ *ste5*Δ cells (our unpublished results). Furthermore, when examined 6 h after galactose addition, cells expressing Ste5(P44L)-GST and Ste5(S770K)-

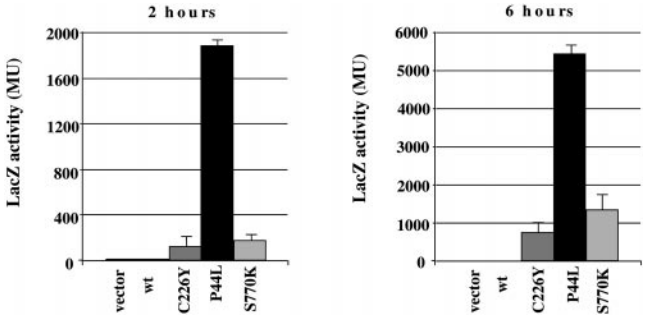

Figure 3. Activated *STE5* alleles stimulate expression of a pheromone-responsive reporter gene. A *ste4*Δ *ste5*Δ strain carrying an empty vector or the same vector expressing wild-type Ste5-GST, or the indicated activated mutant derivatives (as GST fusions), under the control of the *GAL1* promoter, and also cotransformed with a plasmid carrying a *FUS1-lacZ* construct, were pregrown in SCRaf to an $A_{600\ nm} = 0.5$, and then galactose (2% final concentration) was added to induce expression of the proteins. After either 2 h (left) or 6 h (right), cells were collected and assayed for β-galactosidase activity, as described in MATERIALS AND METHODS.

GST displayed a marked increase in volume and formed the pear-shaped morphology with pronounced projections (shmoo tips) that is characteristic of haploid cells treated with pheromone (Figures 2B and 4), whereas cells expressing Ste5(C226Y)-GST enlarged and formed elongated buds, but did not acquire the typical shmoo morphology. Likewise, as revealed by staining with Calcofluor (Figure 2B), chitin deposition was dramatically delocalized in cells expressing Ste5(P44L)-GST and Ste5(S770K)-GST, another hallmark of haploid cells responding to pheromone (Schekman and Brawley, 1979), whereas in cells expressing Ste5(C226Y)-GST, the majority of the chitin was deposited at the incipient division septum in the bud neck, as observed in normally dividing cells (Cabib, 1987).

As an independent and more quantitative measure of the ability of the mutants to activate the pheromone response pathway, the *MAT***a** *ste4*Δ *ste5*Δ cells expressing vector alone, Ste5-GST, and each of the three mutants, were cotransformed with a plasmid carrying a pheromone-responsive reporter gene (*FUS1-lacZ*) (Trueheart *et al.*, 1987) and expression of the proteins was induced by addition of galactose, as before. Two hours after galactose addition, cells carrying vector alone or expressing wild-type Ste5-GST showed only basal levels of β-galactosidase activity; in contrast, cells expressing each of the three mutants showed a pronounced elevation in β-galactosidase activity (Figure 3, left). By this criterion, however, Ste5(P44L)-GST was much more potent (2000-fold induction versus Ste5-GST or vector alone) than either Ste5(S770K)-GST (130-fold induction) or Ste5(C226Y)-GST (100-fold induction). The ability of these activated alleles to induce reporter gene expression was even more evident 6 h after addition of galactose (a time period that correlates well with the appearance of the shmoo-like, or elongated bud, morphology of the corresponding cells) and maintained the same order of potency: P44L (5000-fold induction) > S770K (1300-fold induction) > C226Y (700-fold induction) (Figure 3, right). The level of β-galactosidase expression induced by Ste5(P44L) was ~80% of the level observed in *ste5*Δ cells expressing normal *STE5* in the same manner (under control of a *GAL* promoter on a *CEN* plasmid) and treated with α-factor (15 μM) (our unpublished results).

Nucleocytoplasmic Distribution of Ste5 Is Unaffected by the Activating Mutations

It has been shown that Ste5 shuttles between the nucleus and the cytosol, resides mainly in the nucleus in naive cells, but is exported to the cytoplasm upon pheromone treatment, where it localizes to the protruding shmoo tip via its direct association with Gβγ (Pryciak and Huntress, 1998; Mahanty *et al.*, 1999; Dhillon *et al.*, 2000). Constitutive export of Ste5 from the nucleus seems to require the exportin Xpo1, whereas the enhanced pheromone-induced export seems to require the exportin Msn5/Ste21 (Mahanty *et al.*, 1999; Dhillon *et al.*, 2000). To investigate whether the constitutively active, Gβγ-independent, single-substitution *STE5* alleles identified in this study affect either the default or pheromone-induced localization of Ste5, GFP was fused in-frame to the carboxy-terminus of wild-type Ste5 and each of the three mutant proteins. As in the Ste5-GST fusions, the Ste5(P44L)-GFP, Ste5(S770K)-GFP, and Ste5(C226Y)-GFP chimeras were able to support readily detectable levels of mating in *ste4*Δ *ste5*Δ cells, unlike wild-type Ste5-GFP (our unpublished results). The localization of these Ste5-GFP chimeras was examined in both *ste5*Δ cells (naive and treated with pheromone) and in *ste4*Δ *ste5*Δ cells.

As previously observed, in untreated cells, wild-type Ste5-GFP is predominantly nuclear. As documented elsewhere in detail, the observed localization of Ste5-GFP is not an artifact of its overproduction (Dhillon *et al.*, 2000). Each of the mutant alleles displayed a distribution essentially identical to that observed for wild-type Ste5 (Figure 4, left). Upon pheromone treatment and the release of free Gβγ from the pheromone receptors, wild-type Ste5 rapidly exits the nucleus, such that by 40 min after stimulation, most of the Ste5 is localized to the shmoo tip; likewise, the pheromone-induced translocation and plasma membrane tethering of Ste5(P44L) and Ste5(S770K) seemed to be just as efficient as that of wild-type Ste5 (Figure 4, middle). As observed previously (Pryciak and Huntress, 1998; Dhillon *et al.*, 2000) for other mutations that eliminate or perturb the RING-H2 domain of Ste5 and prevent Ste5–Gβγ interaction (Inouye *et al.*, 1997b; Feng *et al.*, 1998), Ste5(C226Y) could not be stably recruited to the cell membrane after pheromone treatment, suggesting that the C226Y mutation likewise compromises the ability of Ste5 to interact with Gβγ (Figure 4, middle).

In *ste4*Δ *ste5*Δ cells, where Gβγ is absent and the Ste5 mutants display a constitutive ability to signal, all three proteins, like wild-type Ste5, were predominantly nuclear and displayed no detectable hyper-accumulation in the cytosol or at the shmoo tip (Figure 4, right). Thus, these findings indicate, first, that the activated phenotype of these mutants does not result from a change in their subcellular distribution and, second, that stable deposition of Ste5 at the shmoo tip is not essential for the signaling function of Ste5.

Biochemical Characterization of the Activated STE5 Alleles

To determine whether the activating mutations affect the apparent affinity of Ste5 for any of the associated compo-

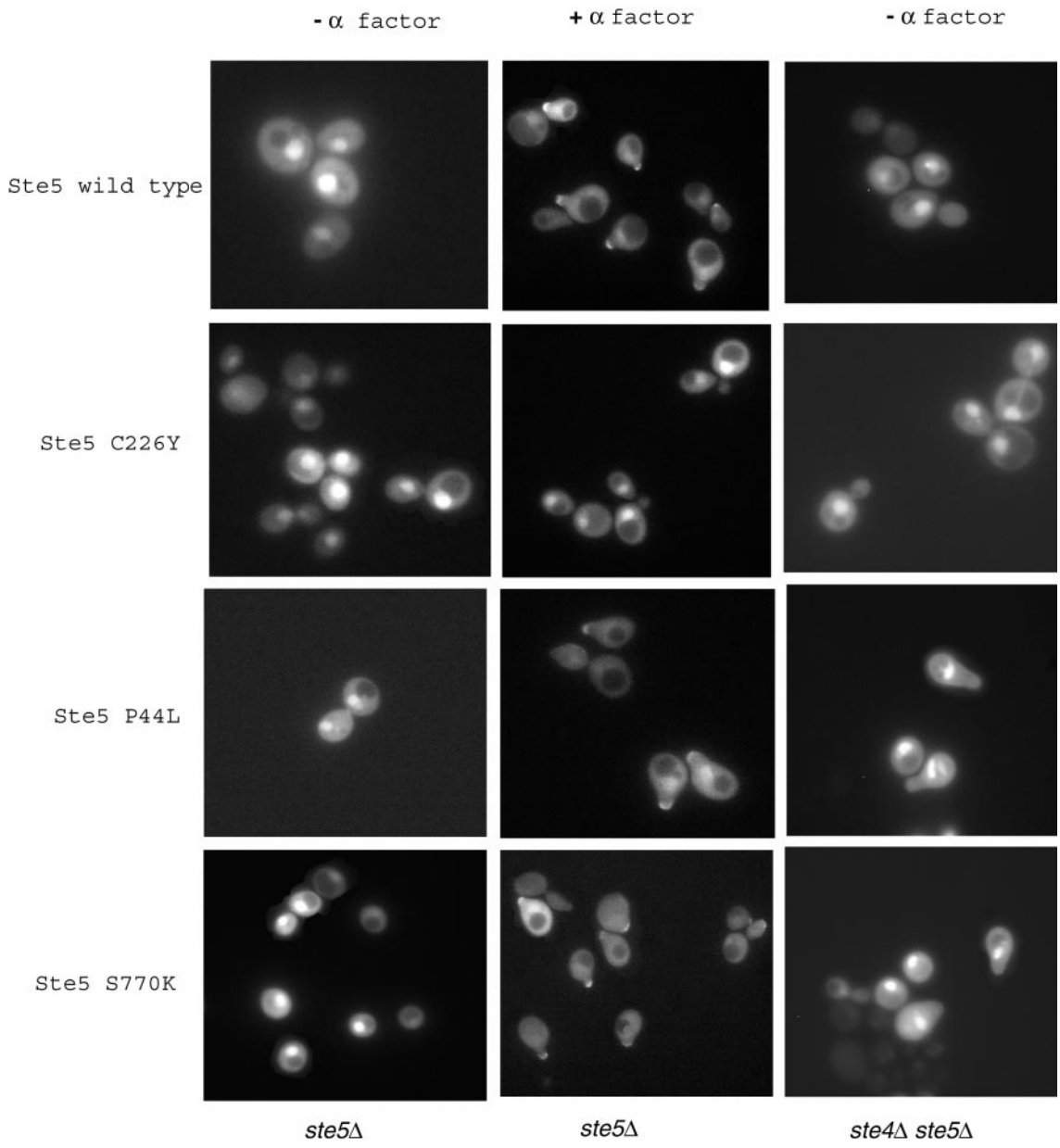

Figure 4. Subcellular localization of wild-type Ste5 and the activated Ste5 mutants. Strain BYB84 (left and middle columns) or strain BYB88 (right column) were transformed with plasmids expressing wild-type Ste5-GFP (pCJ80), Ste5(C226Y)-GFP (pCS49), Ste5(P44L)-GFP (pCS18), or Ste5(S770K)-GFP (pCS50), grown to an $A_{600\ nm}$ = 0.6 in SCRaf medium at 30°C. For BYB88, the cells were also cotransformed with plasmids expressing Ste5-GST (pCJ148), Ste5(C226Y)-GST (pSL1), Ste5(P44L)-GST (pSL2), or Ste5(S770K)-GST (pSL3), as indicated, to promote more robust G$\beta\gamma$-independent shmoo formation. Expression of the Ste5 proteins was then induced by addition of galactose (2% final concentration) followed by incubation for 2–3 h (BYB84) or 4–6 h (BYB88). Induction was terminated by washing the cells in SC medium containing 2% glucose and resuspending them in the same medium. The BYB88 transformants were viewed immediately thereafter under the fluorescence microscope, as described in the legend to Figure 2B, whereas portions of the BYB84 cultures were subjected to pheromone treatment. To retard pheromone proteolysis during pheromone treatment (Ciejek and Thorner, 1979), cultures were adjusted to a final concentration of 25 mM Na-succinate, pH 3.5, before addition of 20 μM α-factor. After 40 min of exposure to pheromone, the cells were viewed by fluorescence microscopy.

nents of the MAPK cascade, extracts were prepared from *MAT***a** *ste4*Δ *ste5*Δ cells carrying vector alone or expressing wild-type Ste5-GST or each of the three single-substitution mutants, which were also tagged with a c-Myc epitope (see MATERIALS AND METHODS), and subjected to immunoprecipitation with a monoclonal antibody directed against this epitope. The amount of Ste11, Ste7, and Fus3 proteins coprecipitated was then assessed by immunoblotting with

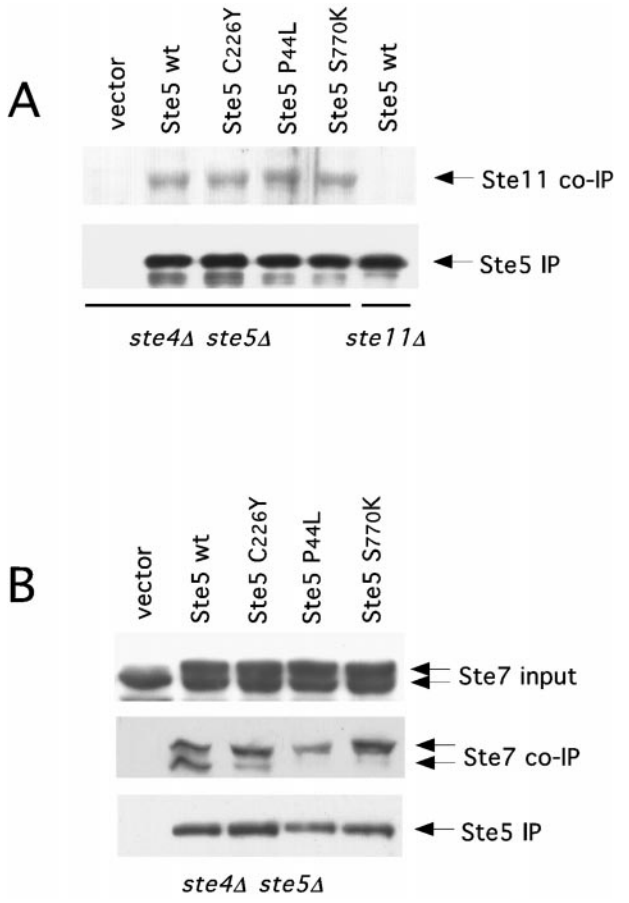

Figure 5. Association of activated Ste5 mutants with Ste11 and Ste7. A *ste4*Δ *ste5*Δ strain was transformed with a vector or with the same vector expressing under the control of the *GAL1* promoter either wild-type *STE5*-GST or the three indicated *STE5*-GST mutants, with or without cotransformation with a plasmid expressing *STE7* from the *GAL1* promoter. The cells were grown to an $A_{600\ nm} = 0.6$ in SCRaf medium at 30°C, and then expression of the Ste5 proteins (with or without Ste7) was induced by addition of galactose (2% final concentration). Three hours after induction, cells were collected and extracts were prepared, as described in MATERIALS AND METHODS. The c-Myc-tagged Ste5-GST proteins were immunoprecipitated with anti-c-Myc monoclonal antibody, and proteins in the bead-bound immune complexes were solubilized, resolved by SDS-PAGE, and analyzed by immunoblotting with the anti-c-Myc antibody ("Ste5 IP") or with anti-Ste11 antibodies to detect the amount of endogenous Ste11 coprecipitated (A) or with anti-Ste7 antibodies to detect the amount of coexpressed Ste7 coprecipitated (B). In (B), samples of the initial extracts ("input") were also analyzed by immunoblotting with the anti-Ste7 antibodies to demonstrate that Ste7 isoforms were expressed at equivalent levels in all of the extracts.

appropriate antibodies after resolution of the immune complexes by SDS-PAGE.

Equivalent amounts of each of the Ste5 proteins were recovered by immunoprecipitation, as judged by immunoblotting (Figure 5). Wild-type Ste5-GST and each of the three mutants coprecipitated similar amounts of endogenous Ste11 (Figure 5A). In some experiments, we noted that the activated alleles, especially Ste5(P44L)-GST and Ste5(S770K)-GST, coprecipitated a doublet of Ste11-related bands rather than a single species (our unpublished results). These bands may represent phosphorylated forms of Ste11, although this possibility was not tested directly.

Because Ste7 is the MAPK cascade component present in the most limiting amounts, it must be overexpressed to be reproducibly detected by immunoblot analysis (Bardwell *et al.*, 1996; Errede and Ge, 1996). Hence, Ste7 was cooverexpressed in the same cells from the *GAL1* promoter on a *CEN* plasmid. As in the case of Ste11, the amount of Ste7 bound to either wild-type Ste5-GST or to the mutants was similar in the majority of experiments (Figure 5B). However, Ste7 exists in both a rapidly migrating hypophosphorylated form and a more slowly migrating hyperphosphorylated form; it has been amply demonstrated that shift to the hyperphosphorylated form is correlated with activation of the pheromone response pathway (Cairns *et al.*, 1992; Zhou *et al.*, 1993). We noted that wild-type Ste5-GST always coprecipitated both forms, whereas both Ste5(P44L)-GST and Ste5(S770K)-GST reproducibly coprecipitated almost exclusively the hyperphosphorylated species, even though both species were present in equivalent amount in the extracts (Figure 5B). In agreement with its less potent activity deduced from phenotypic tests, Ste5(C226Y)-GST displayed an intermediate situation, with both bands present, but with the hyperphosphorylated Ste7 band reproducibly more abundant (Figure 5B).

Hyperphosphorylation of Ste7 requires the MAPKs Fus3 and Kss1 (Cairns *et al.*, 1992; Zhou *et al.*, 1993; Bardwell *et al.*, 1996). Hence, the appearance of the hyperphosphorylated forms of Ste7 bound to the activated Ste5 mutants provided one biochemical confirmation that the MAPKs have become activated in these cells. Indeed, because *FUS3* is a pheromone-responsive gene, activation of this signaling pathway by the mutant Ste5 alleles should lead to overexpression of Fus3, which was observed to be the case as judged by immunoblotting of the extracts (Figure 6A). In contrast to Ste11 and Ste7, all three of the activated Ste5 mutants reproducibly coprecipitated more endogenous Fus3 than Ste5-GST (Figure 6B). However, the greater amount of Fus3 bound to the mutants could merely result from the higher level of Fus3 available. Nonetheless, the Fus3 that coprecipitated with these mutants was more catalytically active than the Fus3 associated with wild-type Ste5-GST (6D), as judged by its ability to phosphorylate a specific substrate, GST-Ste7(1-172) (Figure 6C), even when normalized to the amount of Fus3 coprecipitated (Figure 6E), providing further biochemical confirmation that the constitutively active Ste5 alleles cause activation of the MAPKs. Moreover, both stimulation of Fus3 expression and the level of Fus3 activity displayed the same order of potency among the three alleles as was observed in the phenotype assays: P44L > S770K > C226Y.

Ste5 Activation Enhances MAPK Specific Activity and Requires Ste20 Action

As another approach to confirm that the higher Fus3 activity coprecipitating with the Ste5 mutants was due to a higher specific activity of the enzyme rather than merely reflecting the greater amount of protein bound, the same experiments were performed in a *ste4*Δ *ste5*Δ ste*12*Δ strain. In this back-

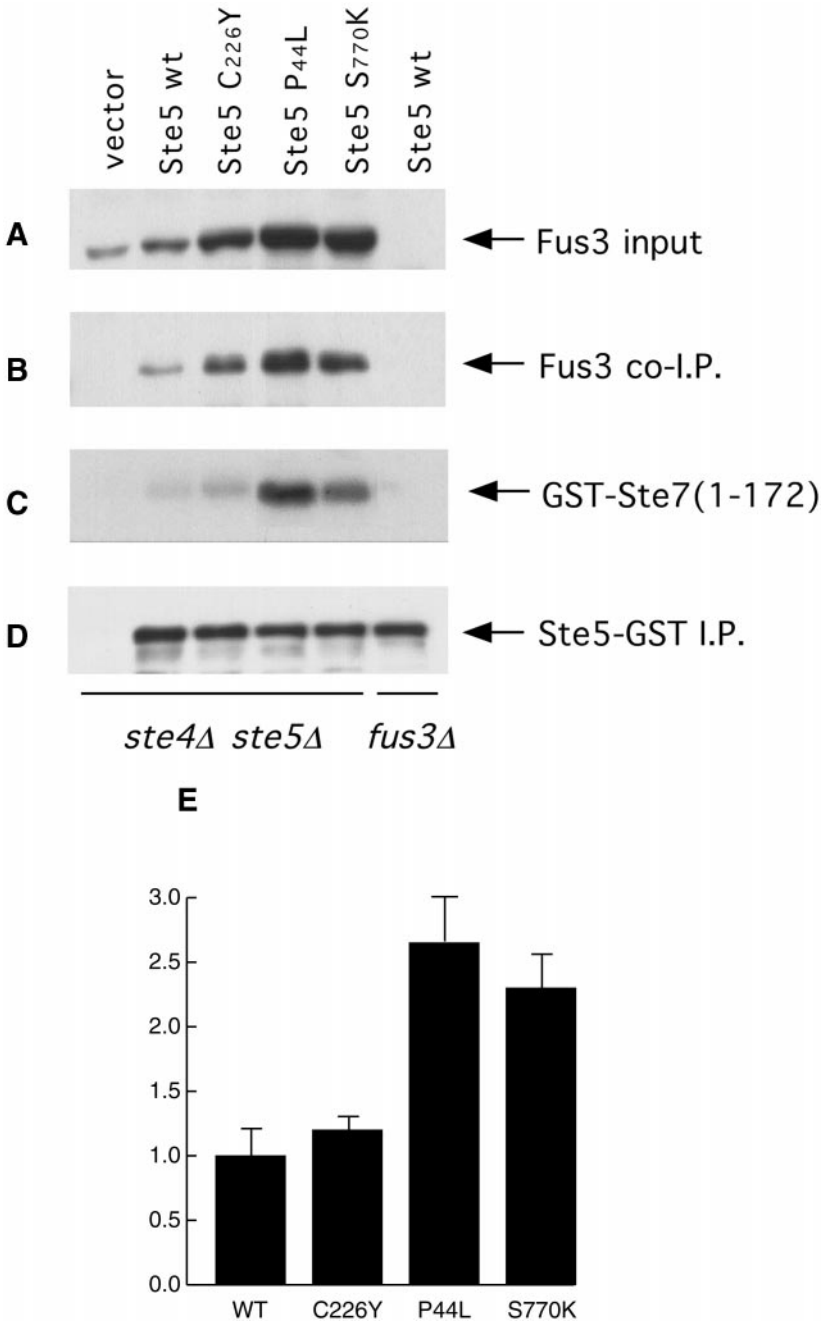

Figure 6. Association of activated Ste5 mutants with Fus3. A *ste4*Δ *ste5*Δ strain was transformed with a vector or with the same vector expressing under the control of the *GAL1* promoter either wild-type *STE5*-GST or the three indicated *STE5*-GST mutants. The cells were grown, induced with galactose, and extracts were prepared, as described in the legend to Figure 5. The c-Myc-tagged Ste5-GST proteins were immunoprecipitated (D) and a portion of the bead-bound immune complexes was analyzed as also described in the legend to Figure 5. The amount of endogenous Fus3 in a sample of each extract ("input") (A) and the amount of endogenous Fus3 that coimmunoprecipitated with Ste5 (B) were assessed by immunoblotting with anti-Fus3 antibodies. (C) A separate portion of the bead-bound immune complexes was washed three times with lysis buffer and twice with kinase assay buffer, and then Fus3 activity present was measured by the incorporation of label into a specific substrate, GST-Ste7(1–172), as described in MATERIALS AND METHODS. (E) Densitometric analysis was performed on the bands in B and C by using NIH imaging software. Values expressed are the ratio of the radiolabel incorporated into substrate in the Fus3 kinase assay (C) to the intensity of the Fus3 protein present in the same coimmunoprecipitates (B), are the average of three independent trials (error bars represent SD of the mean), and are normalized to the value obtained for the immunoprecipitates containing wild-type Ste5.

ground, the lack of the Ste12 transcription factor prevents induction of *FUS3* and other pheromone-regulated genes, even when the pathway becomes activated. Indeed, as expected, equal amounts of Fus3 were present in extracts of cells expressing wild-type Ste5-GST and the three mutants; and, under these conditions, similar amounts of Fus3 now coimmunoprecipitated with the normal Ste5 and the three Ste5 mutants (Figure 7A). However, as judged by the immune-complex kinase assay (Figure 7A), the Fus3 associated with Ste5(P44L)-GST, and to a lesser extent with Ste5(S770K)-GST, reproducibly displayed a higher level of activity than the Fus3 associated with wild-type Ste5-GST (Figure 7A), even when normalized to the amount of Fus3 coprecipitated (Figure 7C), as observed before (Figure 6E). Thus, the constitutively active G$\beta\gamma$-independent mutations in Ste5 act, at least in part, by facilitating activation of the MAPK cascade, even though the effect is seemingly modest ($\leq$2-fold).

To determine whether the constitutive phenotype of the three single-substitution alleles that bypass the need for G$\beta\gamma$ still require the activity of Ste20, a *ste4*Δ *ste5*Δ *ste20*Δ triple mutant strain was generated and *CEN* plasmids expressing

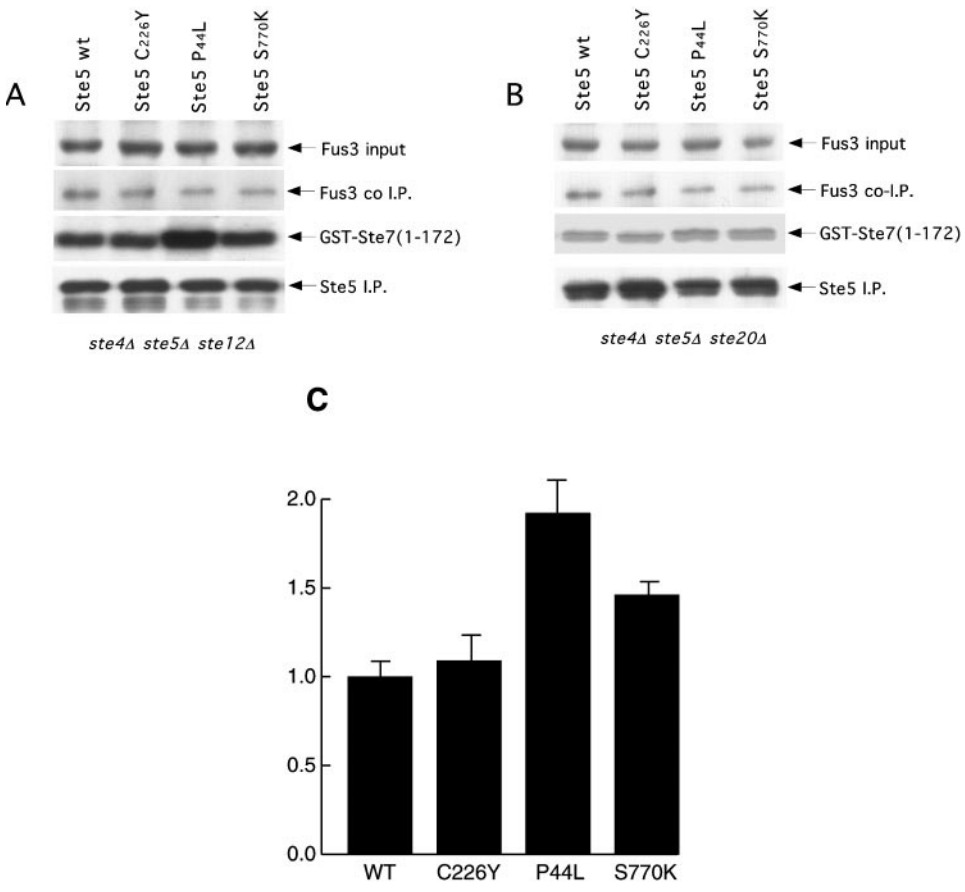

Figure 7. Fus3 associated with activated Ste5 mutants has elevated specific activity that depends on Ste20. The amount of Fus3 in extracts and the amount of Fus3 associated with Ste5, and its enzymic activity, and densitometric analysis, were assessed exactly as described in the legend to Figure 6, except that the cells used were either *ste4*Δ *ste5*Δ *ste12*Δ (A) or *ste4*Δ *ste5*Δ *ste20*Δ (B). Densitometric analysis (C) was performed on the relevant bands in A. Values expressed are the ratio of the radiolabel incorporated into substrate in the Fus3 kinase assay to the intensity of the Fus3 protein present in the same coimmunoprecipitates, are the average of three independent trials (error bars represent SD of the mean), and are normalized to the value obtained for the immunoprecipitates containing wild-type Ste5.

the activated Ste5-GST mutants from the *GAL1* promoter (Figure 1B), as well as 2-μm plasmids expressing the same alleles in the context of *STE5* from the *GAL1* promoter (Figure 1C), were introduced by transformation and tested for their ability to support mating. None of the activated alleles was able to rescue mating in either context when Ste20 was absent (Figure 1, B and C). Correspondingly, at the biochemical level, the MAPK cascade was not activated by any of these mutants when Ste20 was absent, as indicated by the lack of induction of Fus3 expression (Figure 7B) and the low basal activity of the Fus3 associated with the immunoprecipitated Ste5-GST mutants (Figure 7B) (<10% of the activated state, as judged by the exposure time required for autoradiography to detect bands of intensities equivalent to those in Figure 7A; our unpublished results). These results demonstrate that Ste20 is required for the constitutively active phenotype of the G$\beta\gamma$-independent Ste5 mutants and suggest further that, in the normal physiological pathway, Ste20 contributes to Ste5-dependent activation of the MAPK cascade at a stage that occurs after G$\beta\gamma$–Ste5 interaction.

N-terminal and C-terminal Domains of Ste5 Can Physically Interact

What molecular feature of Ste5 is altered by the activating mutations that leads to their ability to stimulate downstream events in the absence of G$\beta\gamma$? The C226Y mutation presumably disrupts the RING-H2 domain, a perturbation that we showed previously alleviates a negative constraint in Ste5 and may mimic a G$\beta\gamma$-induced conformational change (Inouye *et al.*, 1997b). However, we were struck by the fact that the other two single-substitution, gain-of-function alleles we identified lie at opposite ends of the molecule and are situated very near regions of opposite charge. This observation suggested that the N terminus and the C terminus of Ste5 might physically associate with each other, perhaps via electrostatic interactions. To test this possibility, the N-terminal half of Ste5 (residues 1–518) was expressed as a GST fusion protein in *E. coli* and purified by adsorption to glutathione-agarose beads. The C-terminal half of Ste5 (residues 520–917) was prepared in radioactive form by in vitro transcription-translation in a rabbit reticulocyte lysate (Figure 8A, left). To ensure that the purified GST-Ste5(1–518) was folded properly and was competent to bind a protein known to interact with this segment of Ste5 (Figure 1A), radioactive Fus3 was also prepared by in vitro transcription-translation as a positive control (Figure 8A, left).

We found that purified GST-Ste5(1–518) was able to bind both radiolabeled Fus3, as expected, and also Ste5(520–917) (Figure 8A, right), indicating that the N and C termini of Ste5 are able to physically associate in the absence of any other yeast protein. GST alone, which was present in very large excess over the chimeras, as judged by immunoblotting with

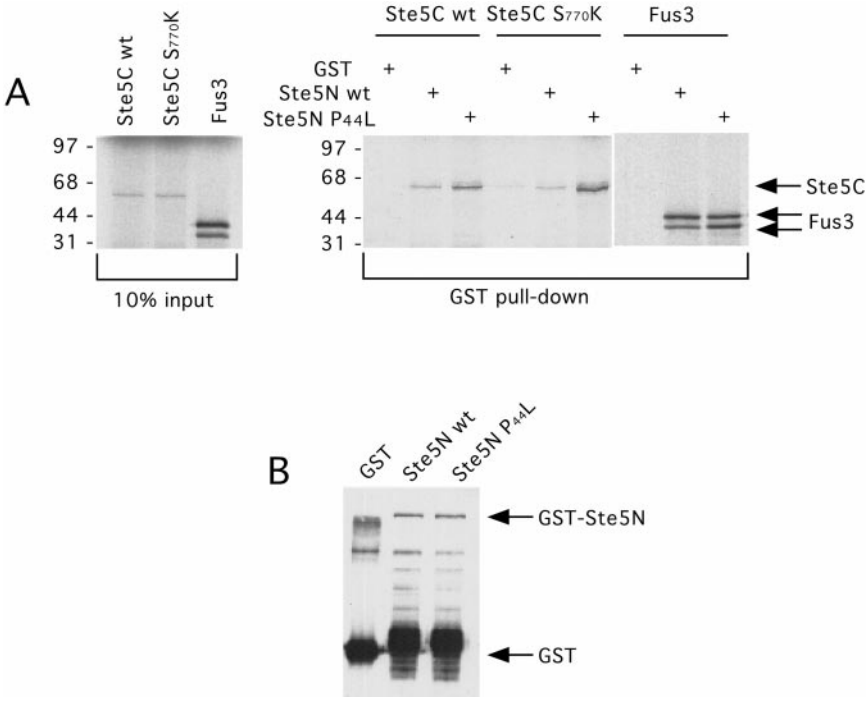

Figure 8. The N and C termini of Ste5 can physically associate. The C-terminal segments (residues 520–917) of wild-type Ste5 and Ste5(S770K), and intact Fus3 were prepared in radiolabeled form by in vitro translation with [^{35}S]methionine and [^{35}S]cysteine and detected by autoradiography (A, left) and incubated, as indicated, with bacterially expressed GST, GST-Ste5(1–518), or GST-Ste5(1–518) carrying the P44L mutation (B) bound on glutathione-agarose beads. GST or GST fusions were detected by immunoblotting with commercial anti-GST antibodies (Santa Cruz Biotechnology). After three washes, bound proteins were eluted with 5 mM reduced glutathione and analyzed by autoradiography after electrophoresis on a 12% SDS-PAGE (A, right).

anti-GST antibodies (Figure 8B), did not bind detectable amounts of either Fus3 or Ste5(520–917), demonstrating that the binding displayed by Ste5(1–518) was specific. To determine whether the P44L and S770K mutations affect this interaction in vitro, GST-Ste5(1–518) containing the P44L mutation was prepared in *E. coli* and Ste5(520–917) containing the S770K mutation was prepared by in vitro translation. Interestingly, GST-Ste5^{P44L}(1–518) bound both the wild-type C-terminal fragment Ste5(520–917) and the mutant C-terminal fragment Ste5^{S770K}(520–917) with higher affinity than did the wild-type N terminus GST-Ste5(1–518) (Figure 8A, right). In contrast, both GST-Ste5(1–518) and GST-Ste5^{P44L}(1–518) bound Fus3 indistinguishably. The best binding was observed between the mutant N-terminal fragment and the mutant C-terminal fragment (Figure 8A, right).

To investigate whether the N-terminal region of Ste5 was able to interact with full-length Ste5 and not just the isolated C-terminal fragment, we performed an independent pull-down experiment by using beads coated with bacterially expressed GST, GST-Ste5^{WT}(1–518), or GST-Ste5^{P44L}(1–518) and extracts of yeast cells expressing either myc-tagged wild-type Ste5, myc-tagged Ste5(P44L), or myc-tagged Ste5(S770K). We found reproducibly that GST-Ste5(1–518) was able to bind full-length Ste5, whereas GST did not (Figure 9A). Furthermore, we found reproducibly that both the P44L and S770K mutations markedly improved binding of full-length Ste5 to the N terminus domain (Figure 9A), corroborating the results obtained with the isolated C-terminal region of Ste5 prepared by in vitro translation (Figure 8).

Because Ste5 has been reported to self-associate (Yablonski *et al.*, 1996; Feng *et al.*, 1998), and this multimerization is thought to be important for signaling (Yablonski *et al.*, 1996; Inouye *et al.*, 1997b), we tested whether the mutations identified in our selection affected Ste5 oligomerization. Differentially tagged Ste5 molecules (Ste5-GST and Ste5-GFP derivatives) were coexpressed in a *ste4*Δ *ste5*Δ strain from the *GAL1* promoter on a *CEN* plasmid, and the Ste5-GST derivatives were immunoprecipitated by using a polyclonal anti-GST antibody. The immunoprecipitates were resolved by SDS-PAGE and the amount of Ste5-GST and coimmunoprecipitated Ste5-GFP were analyzed by immunoblotting with either anti-GST (Figure 9B, top) or anti-GFP (Figure 9B, bottom) antibodies, respectively. In general, for normal Ste5 and each of the three mutants, the amount of Ste5-GFP coprecipitated was in direct proportion to amount of Ste5-GST recovered (Figure 9B). Thus, although Ste5 exists in yeast cell extracts in multimeric form, none of the three activated alleles seemed to strengthen or weaken the efficiency of Ste5–Ste5 interaction assessed in this manner.

Taken together, our results suggest, first, that Ste5 multimerization is constitutive and not involved in the mechanism of activation triggered by the activated alleles. Second, our findings suggest that, rather than promoting more efficient oligomerization per se, both P44L and S770K facilitate signaling in the absence of G$\beta\gamma$ by enhancing association of the N and C termini of Ste5, either within one Ste5 monomer in a preformed oligomer (intramolecular) (Figure 10A) or between two adjacent Ste5 monomers in a preformed oligomer (intermolecular) (Figure 10B).

DISCUSSION

We have identified three mutational alterations in the Ste5 protein that allow it to activate the pheromone response pathway constitutively in the absence of G$\beta\gamma$-dependent stimulation. Using a positive selection (in the context of a

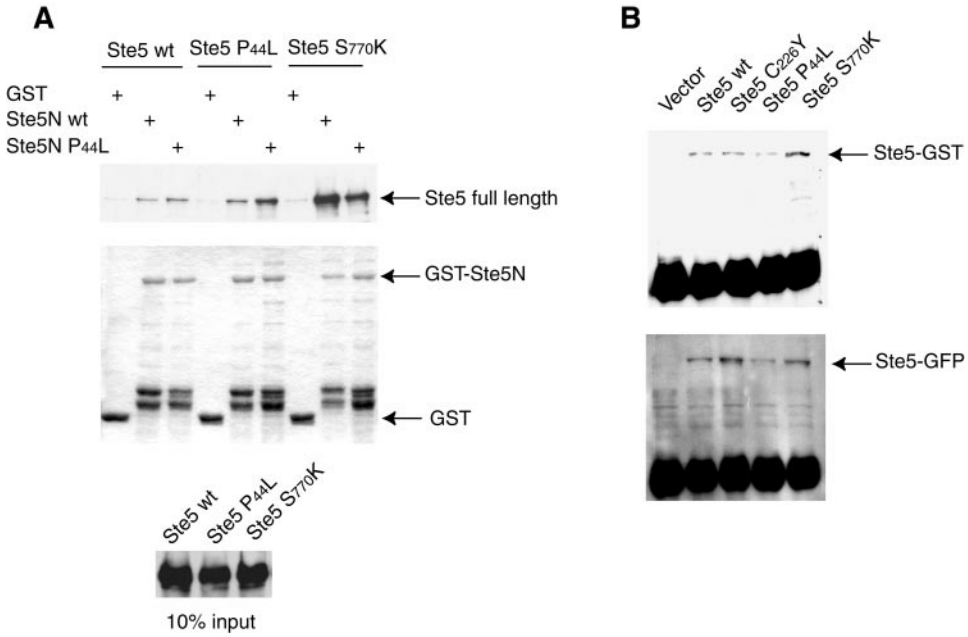

Figure 9. The P44L and S770K mutations enhance binding of full-length Ste5 to the N terminus of Ste5 without affecting Ste5 oligomerization. (A) GST, or GST-Ste5(1–518) ("Ste5N wt"), or GST-Ste5^{P44L}(1–518) ("Ste5N P44L"), as indicated, were expressed and purified from *E. coli*, immobilized on glutathione-agarose beads, as described in the legend to Figure 8, and incubated with extracts from *ste4*Δ *ste5*Δ cells expressing myc-epitope-tagged versions of full-length wild-type Ste5 (Ste5 wt), Ste5(P44L), or Ste5(S770K), as indicated. After three washes, bound proteins were eluted with 5 mM reduced glutathione, resolved by SDS-PAGE, and analyzed either by immunoblotting with anti-Myc monoclonal antibody 9E10 (top) or by Coomassie blue staining (middle). Samples of the initial extracts ("input") were also analyzed by immunoblotting with the anti-Myc antibody to demonstrate that Ste5 and the Ste5 mutants were expressed at equivalent levels in these extracts. (B) Either wild-type Ste5 or the indicated Ste5 mutant (each as a GST fusion) was coexpressed with the same form of Ste5 (as a GFP fusion), each expressed from the *GAL1* promoter on a plasmid, in *ste4*Δ *ste5*Δ cells. Extracts were prepared as described in MATERIALS AND METHODS, and samples (1 mg of total protein) were immunoprecipitated by using polyclonal anti-GST antibodies. Portions of the resulting immunoprecipitates were resolved by SDS-PAGE and examined by immunoblotting with anti-GST antibodies to detect the amount of immunoprecipitated Ste5-GST (top) and with polyclonal anti-GFP antibodies to detect the amount of Ste5-GFP that coimmunoprecipitated (bottom).

Ste5-GST fusion), we identified three single-residue substitution mutations in *STE5* that, by themselves (i.e., even in the absence of fusion to GST), allow for constitutive and G$\beta\gamma$-independent activation of the pheromone response pathway. Each mutation lies in a different region of Ste5. C226Y alters the seventh conserved Zn^{2+}-binding residue in the RING-H2 motif, a domain of Ste5 that mediates its interaction with G$\beta\gamma$ (Inouye *et al.*, 1997b; Pryciak and Huntress, 1998; Feng *et al.*, 1998), contributes to Ste5 oligomerization (Yablonski *et al.*, 1996), and plays an inhibitory role in signaling (Inouye *et al.*, 1997b). This mutation must lift this inhibitory constraint more strongly than the site-directed mutations that we previously made in this same motif because, unlike the C177A C180A allele, the activated phenotype of C226Y did not require its fusion to GST. It is interesting to note that a RING-H2 domain of related sequence mediates the interaction of Far1 with G$\beta\gamma$ (Butty *et al.*, 1998).

P44L resides near the N terminus just upstream of a stretch of basic residues that resembles a bipartite nuclear localization signal. Indeed, it has been reported that removal of this basic segment prevents nuclear entry of Ste5 and compromises Ste5 function (Mahanty *et al.*, 1999). However, in other studies, this segment of Ste5 was not required for its efficient nuclear import (Dhillon *et al.*, 2000). Moreover, as shown here, the P44L mutation does not affect the nucleocytoplasmic distribution of Ste5 in either naive or pheromone-treated cells. Hence, the activating nature of this mutation cannot be attributed to a shift in the subcellular distribution of Ste5. Furthermore, the fact that all three Ste5 mutant proteins remain predominantly nuclear in *ste4*Δ *ste5*Δ cells, where they nonetheless constitutively activate

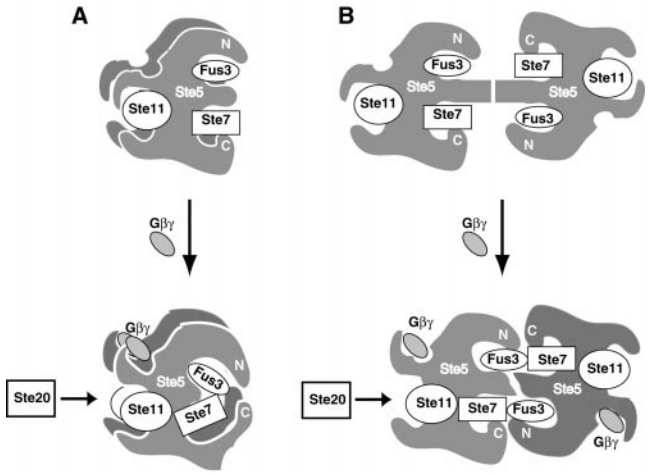

Figure 10. G$\beta\gamma$-induced relief of conformational constraints in Ste5 promotes MAPK activation. The findings obtained in this study suggest a model for how conformational changes in Ste5 contribute to the efficiency of MAPK activation. In naive cells, Ste5 exists as an oligomer (most simply, a dimer) and binds to Ste11, Ste7, and Fus3 in a conformational state that prevents phosphorylation of Ste11 by Ste20. Binding of G$\beta\gamma$ to the RING-H2 domain in Ste5 causes conformational changes that expose Ste11 and permit closer contact between the N and C termini of Ste5, thereby optimizing orientation of the bound kinases for cross-phosphorylation. Collectively, these events facilitating the Ste20-dependent activation of the three kinases of the MAPK module.

the pheromone response pathway, does not support a recent suggestion that cycling of Ste5 from the plasma membrane to the nucleus is necessary for Ste5 to undergo some change (unspecified) by which it acquires a signaling-competent state (Mahanty *et al.*, 1999). As we have demonstrated here, the N-terminal portion of Ste5, which encompasses this basic segment, can interact with the C-terminal portion of Ste5, and the P44L mutation enhanced this interaction. Thus, deletion of the basic segment may block Ste5 function not because it impairs nuclear import but rather because it prevents efficient association of the N and C termini.

S770K resides just proximal to an extended stretch of acidic residues within a rather large region (residues 744–895) required for binding of the MEK Ste7. However, neither Ste5(S770K) nor the other two mutants caused any detectable change in affinity for Ste7 or the other two bound kinases. Rather, like the P44L mutation, the S770K mutation enhanced the N–C interaction in Ste5. Moreover, as judged by the state of both Ste7 and Fus3, both activated Ste5 mutants copurified (as GST fusions) with components of the MAPK cascade in their activated forms. This observation provides confirmation that these activated alleles of Ste5 cause activation of the MAPK cascade and indicate further that these mutations must facilitate signaling.

By what mechanism do these single-residue changes in Ste5 promote signaling? The fact that one allele (P44L) fell in a basic region at the N terminus, another (S770K) was situated near an acidic tract at the C terminus, and the third (C226Y) resided in a domain flanked by proline-rich regions that could serve as "hinges," suggested that the N and C termini of Ste5 might physically associate. We were able to demonstrate this interaction and found that these mutations enhance (rather than disrupt) this interaction. Therefore, because Fus3 binds near the N terminus of Ste5 and Ste7 binds to the C terminus of Ste5 (Choi *et al.*, 1994; Inouye *et al.*, 1997a), we propose that association of these domains (either intermolecularly or intramolecularly) permits more intimate contact between the MEK and its target MAPK (Figure 10).

The gain-of-function Ste5 mutations identified in the present work stimulated the mating pathway in the absence of pheromone stimulation and in the absence of G$\beta\gamma$, as demonstrated by a variety of criteria, including imposition of G_1 arrest, acquisition of altered morphology, increased expression of a reporter gene under control of a pheromone-responsive promoter (*FUS1*), elevated expression of an endogenous pheromone-inducible gene (*FUS3*), hyperphosphorylation of Ste7, and enhanced activity of the associated MAPK in vitro. In all phenotypic and biochemical tests applied, the P44L mutation always conferred the strongest phenotype, followed by the S770K mutation, with the C226Y mutation conferring the mildest effects.

Interestingly, the morphological changes induced by both Ste5(P44L) and Ste5(S770K) in *ste4*Δ *ste5*Δ cells (Figure 4) resemble in all respects examined the shmoo-like forms normally seen after pheromone treatment of wild-type haploids (reviewed in Leberer *et al.*, 1997a; Madden and Snyder, 1998; Chant, 1999). Because these morphological changes are occurring in the total absence of G$\beta\gamma$, components other than those thought to be recruited to the shmoo tip via interaction with G$\beta\gamma$, including Ste20 (Leeuw *et al.*, 1998) and Far1 (Butty *et al.*, 1998; Nern and Arkowitz, 1999), must be able to mediate polarization of the actin cytoskeleton. In addition to the scaffold protein Far1 (Valtz *et al.*, 1995), this morphological change normally involves the small GTPase Cdc42 (Johnson, 1999), its guanine-nucleotide exchange factor Cdc24 (Zheng *et al.*, 1994), and a protein containing two SH3 domains, Bem1 (Chenevert *et al.*, 1992). Similarly to Ste5, it has been shown recently that Far1 and Cdc24 are relocalized from the nucleus to the cytoplasm upon pheromone treatment (Blondel *et al.*, 1999; Toenjes *et al.*, 1999; Shimada *et al.*, 2000). Because this translocation event requires an intact MAPK cascade (Butty *et al.*, 1998), it is possible that our constitutive Ste5 mutants induce relocalization of Far1 and thereby activate actin polymerization. Although G$\beta\gamma$ is responsible for tethering Far1 at the shmoo tip in normal cells, we have shown that the activated Ste5 alleles can induce shmoo formation even in G$\beta\gamma$-deficient cells. Hence, other factors must be able to act as landmarks for establishment of the site of polarized growth of the actin cytoskeleton. In this regard, Bem1 has been shown to interact with Ste5 (Leeuw *et al.*, 1995; Lyons *et al.*, 1996), although the function of this interaction is unknown, and is localized to the shmoo tip in pheromone-treated cells (Ayscough and Drubin, 1998). The RING-H2 motif in Ste5 (residues 177–229) is flanked on both its proximal and distal sides by Pro-rich regions (residues 5–162 and residues 260–337, respectively) that could serve as appropriate target sites for binding SH3 domains. Moreover, both an activated allele we previously identified, Ste5(T52M) (Hasson *et al.*, 1994), and the Ste(P44L) allele described here, are located within the first Pro-rich region. Collectively, these observations suggest that Ste5 has a function in the branch of the pheromone response pathway that leads to changes in morphology as well as in the branch that leads to activation of the MAPK cascade. Thus, Ste5 clearly plays a more active role in signaling than a passive scaffold that simply holds Ste11, Ste7, and Fus3 in proximity and shields them from inadvertant activation.

The mechanism of activation of the MAPK cascade in response to the pheromone-induced release of G$\beta\gamma$ is not completely understood. Several lines of evidence indicate that both Ste5 and Ste20 are required for activation of the MEKK, Ste11 (reviewed in Gustin *et al.*, 1998; Posas *et al.*, 1998). Cells lacking Ste5 are completely sterile (Hartwell, 1980), whereas cells lacking Ste20 mate at a detectable, albeit dramatically decreased, efficiency (Leberer *et al.*, 1992, 1993). These observations led to a hypothesis that Ste5 activates the MAPK cascade via both a Ste20-dependent and a Ste20-independent mechanism (Lyons *et al.*, 1996). The activated alleles of *STE5* we have described here do not bind components of the MAPK cascade more avidly, but do bind them in their activated state. Thus, these mutants presumably mimic a conformational state of Ste5 that is normally induced via its interaction with G$\beta\gamma$, thereby enhancing the accessibility of Ste11 to phosphorylation by Ste20 (Figure 10). It is possible that Ste20-dependent phosphorylation of Ste5 itself helps reinforce or further promotes access of Ste20 to Ste11 because we have observed that Ste5 is a target of Ste20-mediated phosphorylation in vitro (C. Sette and J. Thorner, unpublished results). In any event, the results we have presented here clearly demonstrate that the hyperactive Ste5 alleles can only activate the mating response in *ste4*Δ *ste5*Δ cells when Ste20 is present, suggesting either that there is no Ste20-independent route for Ste11 activation or,

less likely, that Ste20-independent activation of Ste11 requires the presence of G$\beta\gamma$.

In naive cells, Ste5 is mainly nuclear (Pryciak and Huntress, 1998; Mahanty *et al.*, 1999; Dhillon *et al.*, 2000), whereas Ste20 is present at the plasma membrane by virtue of its interaction with Cdc42 (Peter *et al.*, 1996; Leberer *et al.*, 1997b). Pheromone induces translocation of Ste5 from the nucleus to the shmoo tip, in a manner that depends on the availability of free G$\beta\gamma$ (Pryciak and Huntress, 1998; Mahanty *et al.*, 1999; Dhillon *et al.*, 2000). Because G$\beta\gamma$ also interacts with Ste20 in a pheromone-dependent manner (Leeuw *et al.*, 1998), it has been proposed that the released G$\beta\gamma$ recruits Ste5 and Ste20, and tethers them in close juxtaposition (Leeuw *et al.*, 1998; Pryciak and Huntress, 1998). Because Ste5 interacts with G$\beta\gamma$ through its RING-H2 domain, and mutation of residues in the consensus residues of this motif (C177 C180 and C226) activate Ste5 (especially in the context of a GST fusion), the RING-H2 domain may impose some structural constraint in Ste5 that prevents Ste20-dependent activation of Ste11 (Figure 10). This model explains how conformational change in Ste5 (induced normally by interaction with G$\beta\gamma$ or artificially by the mutations we have identified) could facilitate Ste20-dependent activation of Ste11.

In further support of the conclusion that the G$\beta\gamma$–Ste5 interaction induces a global rearrangement in the structure of Ste5, we identified and characterized here mutations at opposite ends of the primary structure of the polypeptide that hyperactivate Ste5 even more strongly than do alterations of the RING-H2 domain. Therefore, it seems likely that in its inactive state Ste5 anchors the three MAPK components to different domains in a conformation that prevents their interaction and phosphorylation. Upon pheromone stimulation, G$\beta\gamma$ interaction with Ste5 must cause a rearrangement that allows not only access of Ste20 to Ste11 but also places the three protein kinases in relative orientations that permit their productive cross-phosphorylation (Figure 10). In agreement with this supposition, we found that the activated Ste5 mutants copurified with Ste7 and Fus3 in their activated states. Moreover, we found that the N and C termini of Ste5 are able to interact with each other, when expressed as separate proteins or in the context of full-length Ste5, and that the mutations that activate Ste5 for signaling enhanced this interaction. Thus, G$\beta\gamma$ binding to Ste5 presumably promotes this N–C interaction. From our experiments, however, we cannot determine whether this N–C interaction occurs intramolecularly within a Ste5 monomer or intermolecularly between two Ste5 monomers (Figure 10).

ACKNOWLEDGMENTS

We thank Gustav Ammerer, Sandy Ramer, and Ron Davis for supplying plasmids; Brad Cairns, Julie Brill, and Gerry Fink for providing antibodies; Markus Künzler for the communication of unpublished results; and Judy Shimoni, Victor Cid, and other members of the Thorner Lab for reagents, advice, and other material assistance. This work was supported by a postdoctoral fellowship from the American-Italian Cancer Research Foundation (to C.S.), by a postdoctoral fellowship from the American Cancer Society (to C.J.I.), by a predoctoral fellowship from the National Science Foundation (to S.S.), by National Institutes of Health Research Grant GM-21841 (to J.T.) and by facilities provided the Berkeley campus Cancer Research Laboratory.

REFERENCES

Ayscough, K.R., and Drubin, D.G. (1998). A role for the yeast actin cytoskeleton in pheromone receptor clustering and signaling. Curr. Biol. *8*, 927–930.

Bardwell, L., Cook, J.G., Chang, E.C., Cairns, B.R., and Thorner, J. (1996). Signaling in the yeast pheromone response pathway: specific and high-affinity interaction of the mitogen-activated protein (M.A.P) kinases Kss1 and Fus3 with the upstream M.A.P. kinase kinase Ste7. Mol. Cell. Biol. *16*, 3637–3650.

Bardwell, L., Cook, J.G., Inouye, C.J., and Thorner, J. (1994). Signal propagation and regulation in the mating pheromone response pathway of the yeast *Saccharomyces cerevisiae.* Dev. Biol. *166*, 363–379.

Bardwell, L., Cook, J.G., Zhu-Shimoni, J.X., Voora, D., and Thorner, J. (1998). Differential regulation of transcription: repression by unactivated mitogen-activated protein kinase Kss1 requires the Dig1 and Dig2 proteins. Proc. Natl. Acad. Sci. USA *95*, 15400–15405.

Biggin, M.D., Gibson, T.J., and Hong, G.F. (1983). Buffer gradient gels and ^{35}S label as an aid to rapid DNA sequence determination. Proc. Natl. Acad. Sci. USA *80*, 3963–3965.

Blondel, M., Alepuz, P.M., Huang, L.S., Shaham, S., Ammerer, G., and Peter, M. (1999). Nuclear export of Far1p in response to pheromones requires the export receptor Msn5p/Ste21p. Genes Dev. *13*, 2284–2300.

Brill, J.A., Elion, E.A., and Fink, G.R. (1994). A role for autophosphorylation revealed by activated alleles of FUS3, the yeast MAP kinase homolog. Mol. Biol. Cell *5*, 297–312.

Butty, A.C., Pryciak, P.M., Huang, L.S., Herskowitz, I., and Peter, M. (1998). The role of Far1p in linking the heterotrimeric G protein to polarity establishment proteins during yeast mating. Science *282*, 1511–1516.

Cabib, E. (1987). The synthesis and degradation of chitin. Adv. Enzymol. 59, 59–101.

Cairns, B.R., Ramer, S.W., and Kornberg, R.D. (1992). Order of action of components in the yeast pheromone response pathway revealed with a dominant allele of the STE11 kinase and the multiple phosphorylation of the STE7 kinase. Genes Dev. *6*, 1305–1318.

Chant, J. (1999). Cell polarity in yeast. Annu. Rev. Cell Dev. Biol. *15*, 365–391.

Chenevert, J., Corrado, K., Bender, A., Pringle, J., and Herskowitz, I. (1992). A yeast gene (BEM1) necessary for cell polarization whose product contains two SH3 domains. Nature *356*, 77–79.

Choi, K.Y., Satterberg, B., Lyons, D.M., and Elion, E.A. (1994). Ste5 tethers multiple protein kinases in the MAP kinase cascade required for mating in *S. cerevisiae*. Cell *78*, 499–512.

Ciejek, E., and Thorner, J. (1979). Recovery of *S. cerevisiae* a cells from G1 arrest by alpha factor pheromone requires endopeptidase action. Cell *18*, 623–635.

Cook, J.G., Bardwell, L., Kron, S.J., and Thorner, J. (1996). Two novel targets of the MAP kinase Kss1 are negative regulators of invasive growth in the yeast *Saccharomyces cerevisiae.* Genes Dev. *10*, 2831–2848.

Dhillon, N., Inouye, C.J., Sette, C., Macara, I.G., and Thorner, J. (2000). Nuclear translocation and plasma membrane tethering of the Ste5 scaffold protein during pheromone response in the yeast *Saccharomyces cerevisiae.* J. Cell Biol., in press.

Dowell, S.J., Bishop, A.L., Dyos, S.L., Brown, A.J., and Whiteway, M.S. (1999). Mapping of a yeast G protein beta-gamma signaling interaction. Genetics *150*, 1407–1417.

Drogen, F., O'Rourke, S.M., Stucke, V.M., and Jaquenoud, M. (2000). Phosphorylation of the MEKK Ste11p by the PAK-like kinase Ste20p

is required for MAP kinase signaling in vivo. Curr. Biol. *10*, 630–639.

Elion, E.A. (1995). Ste5 - a meeting place for MAP kinases and their associates. Trends Cell Biol. *5*, 322–327.

Elion, E.A., Satterberg, B., and Kranz, J.E. (1993). FUS3 phosphorylates multiple components of the mating signal transduction cascade: evidence for STE12 and FAR1. Mol. Biol. Cell *4*, 495–510.

Erdman, S., Lin, L., Malczynski, M., and Snyder, M. (1998). Pheromone-regulated genes required for yeast mating differentiation. J. Cell Biol. *140*, 461–483.

Errede, B., and Ge, Q.Y. (1996). Feedback regulation of MAP kinase signal pathways. Philos. Trans. R. Soc. Lond. B *351*, 143–149.

Evan, G.I., Lewis, G.K., Ramsay, G., and Bishop, J.M. (1985). Isolation of monoclonal antibodies specific for human c-myc proto-oncogene product. Mol. Cell. Biol. *5*, 3610–3616.

Feng, Y., Song, L.Y., Kincaid, E., Mahanty, S.K., and Elion, E.A. (1998). Functional binding between Gbeta and the LIM domain of Ste5 is required to activate the MEKK Ste11. Curr. Biol. *8*, 267–278.

Gustin, M.C., Albertyn, J., Alexander, M., and Davenport, K. (1998). MAP kinase pathways in the yeast *Saccharomyces cerevisiae.* Microbiol. Mol. Biol. Rev. *62*, 1264–1300.

Hanahan, D. (1983). Studies on transformation of *Escherichia coli* with plasmids. J. Mol. Biol. *166*, 557–580.

Hartwell, L.H. (1980). Mutants of *Saccharomyces cerevisiae* unresponsive to cell division control by polypeptide mating hormone. J. Cell Biol. *85*, 811–822.

Hasson, M.S., Blinder, D., Thorner, J., and Jenness, D.D. (1994). Mutational activation of the *STE5* gene product bypasses the requirement for G protein beta and gamma subunits in the yeast pheromone response pathway. Mol. Cell. Biol. *14*, 1054–1065.

Hirschman, J.E., and Jenness, D.D. (1999). Dual lipid modification of the yeast gamma subunit Ste18p determines membrane localization of Gbeta/gamma. Mol. Cell. Biol. *19*, 7705–7711.

Hung, W., Olson, K.A., Breitkreutz, A., and Sadowski, I. (1997). Characterization of the basal and pheromone-stimulated phosphorylation states of Ste12p. Eur. J. Biochem. *245*, 241–251.

Inouye, C., Dhillon, N., Durfee, T., Zambryski, P.C., and Thorner, J. (1997a). Mutational analysis of STE5 in the yeast *Saccharomyces cerevisiae*: application of a differential interaction trap assay for examining protein-protein interactions. Genetics *147*, 479–92.

Inouye, C., Dhillon, N., and Thorner, J. (1997b). Ste5 RING-H2 domain: role in Ste4-promoted oligomerization for yeast pheromone signaling. Science *278*, 103–106.

Johnson, D.I. (1999). Cdc42: an essential Rho-type GTPase controlling eukaryotic cell polarity. Microbiol. Mol. Biol. Rev. *63*, 54–105.

Jones, J.S., and Prakash, L. (1990). Yeast *Saccharomyces cerevisiae* selectable markers in pUC18 polylinkers. Yeast *6*, 363–366.

Leberer, E., Dignard, D., Harcus, D., Hougan, L., Whiteway, M., and Thomas, D.Y. (1993). Cloning of *Saccharomyces cerevisiae* STE5 as a suppressor of a Ste20 protein kinase mutant: structural and functional similarity of Ste5 to Far1. Mol. Gen. Genet. *241*, 241–254.

Leberer, E., Dignard, D., Harcus, D., Thomas, D.Y., and Whiteway, M. (1992). The protein kinase homologue Ste20p is required to link the yeast pheromone response G-protein beta gamma subunits to downstream signaling components. EMBO J. *11*, 4815–4824.

Leberer, E., Thomas, D.Y., and Whiteway, M. (1997a). Pheromone signaling and polarized morphogenesis in yeast. Curr. Opin. Genet. Dev. *7*, 59–66.

Leberer, E., Wu, C., Leeuw, T., Fourest-Lieuvin, A., Segall, J.E., and Thomas, D.Y. (1997b). Functional characterization of the Cdc42p binding domain of yeast Ste20p protein kinase. EMBO J. *16*, 83–97.

Leeuw, T., Fourest-Lieuvin, A., Wu, C., Chenevert, J., Clark, K., Whiteway, M., Thomas, D.Y., and Leberer, E. (1995). Pheromone response in yeast: association of Bem1p with proteins of the MAP kinase cascade and actin. Science *270*, 1210–1213.

Leeuw, T., Wu, C., Schrag, J.D., Whiteway, M., Thomas, D.Y., and Leberer, E. (1998). Interaction of a G-protein beta-subunit with a conserved sequence in Ste20/PAK family protein kinases. Nature *391*, 191–195.

Lyons, D.M., Mahanty, S.K., Choi, K.Y., Manandhar, M., and Elion, E.A. (1996). The SH3-domain protein Bem1 coordinates mitogen-activated protein kinase cascade activation with cell cycle control in *Saccharomyces cerevisiae.* Mol. Cell. Biol. *16*, 4095–4106.

Madden, K., and Snyder, M. (1998). Cell polarity and morphogenesis in budding yeast. Annu. Rev. Microbiol. *52*, 687–744.

Madhani, H.D., Galitski, T., Lander, E.S., and Fink, G.R. (1999). Effectors of a developmental mitogen-activated protein kinase cascade revealed by expression signatures of signaling mutants. Proc. Natl. Acad. Sci. USA *96*, 12530–12535.

Mahanty, S.K., Wang, Y., Farley, F.W., and Elion, E.A. (1999). Nuclear shuttling of yeast scaffold Ste5 is required for its recruitment to the plasma membrane and activation of the mating MAPK cascade. Cell *98*, 501–512.

Manahan, C.L., Patnana, M., Blumer, K.J., and Linder, M.E. (2000). Dual lipid modification motifs in Galpha and Ggamma are required for full activity of the pheromone response pathway in *Saccharomyces cerevisiae*. Mol. Biol. Cell. *11*, :957–968.

Manser, E., and Lim, L. (1999). Roles of PAK family kinases. Prog. Mol. Subcell. Biol. *22*, 115–133.

Marcus, S., Polverino, A., Barr, M., and Wigler, M. (1994). Complexes between Ste5 and components of the pheromone-responsive mitogen-activated protein kinase module. Proc. Natl. Acad. Sci. USA *91*, 7762–7766.

Maru, Y., Afar, D.E., Witte, O.N., and Shibuya, M. (1996). The dimerization property of glutathione S-transferase partially reactivates Bcr-Abl lacking the oligomerization domain. J. Biol. Chem. *271*, 15353–15357.

Neiman, A.M., and Herskowitz, I. (1994). Reconstitution of a yeast protein kinase cascade in vitro: activation of the yeast MEK homologue STE7 by STE11. Proc. Natl. Acad. Sci. USA *91*, 3398–3402.

Nern, A., and Arkowitz, R.A. (1999). A Cdc24p-Far1p-Gbeta-gamma protein complex required for yeast orientation during mating. J. Cell Biol. *144*, 1187–1202.

Peter, M., Gartner, A., Horecka, J., Ammerer, G., and Herskowitz, I. (1993). FAR1 links the signal transduction pathway to the cell cycle machinery in yeast. Cell *73*, 747–760.

Peter, M., and Herskowitz, I. (1994). Direct inhibition of the yeast cyclin-dependent kinase Cdc28-Cln by Far1. Science *265*, 1228–1231.

Peter, M., Neiman, A.M., Park, H.O., van Lohuizen, M., and Herskowitz, I. (1996). Functional analysis of the interaction between the small GTP binding protein Cdc42 and the Ste20 protein kinase in yeast. EMBO J. *15*, 7046–7059.

Posas, F., and Saito, H. (1997). Osmotic activation of the HOG MAPK pathway via Ste11p MAPKKK: scaffold role of Pbs2p MAPKK. Science *276*, 1702–1705.

Posas, F., Takekawa, M., and Saito, H. (1998). Signal transduction by MAP kinase cascades in budding yeast. Curr. Opin. Microbiol. *1*, 175–182.

Pringle, J.R., Adams, A.E.M., Drubin, D.G., and Haarer, B.K. (1991). Immuno-fluorescence methods for yeast. Methods Enzymol. *194*, 565–602.

Printen, J.A., and Sprague, G.F. (1994). Protein-protein interactions in the yeast pheromone response pathway—Ste5p interacts with all members of the MAP kinase cascade. Genetics *138*, 609–619.

Pryciak, P.M., and Huntress, F.A. (1998). Membrane recruitment of the kinase cascade scaffold protein Ste5 by the Gbeta/gamma complex underlies activation of the yeast pheromone response pathway. Genes Dev. *12*, 2684–2697.

Ramer, S.W., and Davis, R.W. (1993). A dominant truncation allele identifies a gene, STE20, that encodes a putative protein kinase necessary for mating in *Saccharomyces cerevisiae.* Proc. Natl. Acad. Sci. USA *90*, 452–456.

Roberts, C.J., B. Nelson, M.J. Marton, R. Stoughton, M.R. Meyer, H.A. Bennett, Y.D. He, H. Dai, W.L. Walker, T.R. Hughes, M. Tyors, C. Bione, and S. H. Friend. 2000. Signaling and circuitry of multiple MAPK pathways revealed by a matrix of global gene expression profiles. Science *287*, 873–880.

Rothstein, R.J. (1983). One-step gene disruption in yeast. Methods Enzymol. *101*, 202–211.

Sambrook, J., Fritsch, E.F., and Maniatis, T. (1989). Molecular Cloning: A Laboratory Manual, 2nd ed., Cold Spring Harbor, NY: Cold Spring Harbor Laboratory.

Schekman, R., and Brawley, V. (1979). Localized deposition of chitin on the yeast cell surface in response to mating pheromone. Proc. Natl. Acad. Sci. USA *76*, 645–649.

Sherman, F., Fink, G.R., and Hicks, J.B. (1986). A Laboratory Course Manual for Methods in Yeast Genetics. Cold Spring Harbor, NY: Cold Spring Harbor Laboratory.

Shimada, Y., Gulli, M.-P., and Peter, M. (2000). Nuclear sequestration of the exchange factor Cdc24 by Far1 regulates cell polarity during yeast mating. Nat. Cell Biol. *2*, 117–124.

Song, D., Dolan, J.W., Yuan, Y.L., and Fields, S. (1991). Pheromone-dependent phosphorylation of the yeast STE12 protein correlates with transcriptional activation. Genes Dev. *5*, 741–750.

Sprague, G.F.J. (1991). Assay of yeast mating reaction. Methods Enzymol. *194*, 77–93.

Tedford, K., Kim, S., Sa, D., Stevens, K., and Tyers, M. (1997). Regulation of the mating pheromone and invasive growth responses in yeast by two MAP kinase substrates. Curr. Biol. *7*, 228–238.

Toenjes, K.A., Sawyer, M.M., and Johnson, D.I. (1999). The guanine-nucleotide-exchange factor Cdc24p is targeted to the nucleus and polarized growth sites. Curr. Biol. *9*, 1183–1186.

Trueheart, J., Boeke, J.D., and Fink, G.R. (1987). Two genes required for cell fusion during yeast conjugation: evidence for a pheromone-induced surface protein. Mol. Cell. Biol. *7*, 2316–2328.

Tyers, M., and Futcher, B. (1993). Far1 and Fus3 link the mating pheromone signal transduction pathway to three G1-phase Cdc28 kinase complexes. Mol. Cell. Biol. *13*, 5659–5669.

Valtz, N., Peter, M., and Herskowitz, I. (1995). FAR1 is required for oriented polarization of yeast cells in response to mating pheromones. J. Cell Biol. *131*, 863–873.

Whiteway, M.S., Wu, C., Leeuw, T., Clark, K., Fourest-Lieuvin, A., Thomas, D.Y., and Leberer, E. (1995). Association of the yeast pheromone response G protein beta gamma subunits with the MAP kinase scaffold Ste5p. Science *269*, 1572–1575.

Wu, C., Whiteway, M., Thomas, D.Y., and Leberer, E. (1995). Molecular characterization of Ste20p, a potential mitogen-activated protein or extracellular signal-regulated kinase kinase kinase (MEKK) kinase from *Saccharomyces cerevisiae.* J. Biol. Chem. *270*, 15984–15992.

Yablonski, D., Marbach, I., and Levitzki, A. (1996). Dimerization of Ste5, a mitogen-activated protein kinase cascade scaffold protein, is required for signal transduction. Proc. Natl. Acad. Sci. USA *93*, 13864–13869.

Yashar, B., Irie, K., Printen, J.A., Stevenson, B.J., Sprague, G.F.J., Matsumoto, K., and Errede, B. (1995). Yeast MEK-dependent signal transduction: response thresholds and parameters affecting fidelity. Mol. Cell. Biol. *15*, 6545–6553.

Zheng, Y., Cerione, R., and Bender, A. (1994). Control of the yeast bud-site assembly GTPase Cdc42. Catalysis of guanine nucleotide exchange by Cdc24 and stimulation of GTPase activity by Bem3. J. Biol. Chem. *269*, 2369–2372.

Zhou, Z., Gartner, A., Cade, R., Ammerer, G., and Errede, B. (1993). Pheromone-induced signal transduction in *Saccharomyces cerevisiae* requires the sequential function of three protein kinases. Mol. Cell. Biol. *13*, 2069–2080.